Elimination of reference mapping bias reveals robust immune related allele-specific expression in cross-bred sheep

Mazdak Salavati [1*], Stephen J. Bush [1], Sergio Palma-Vera [2], Mary E.B. McCulloch [1], David A. Hume [3] and Emily L. Clark [1*]

1. The Roslin Institute and Royal (Dick) School of Veterinary Studies, University of Edinburgh, Easter Bush, Midlothian, UK
2. Leibniz Institute for Farm Animal Biology (FBN), Dummerstorf, Germany
3. Mater Research Institute-University of Queensland, Translational Research Institute, Woolloongabba, Qld 4102, Australia

*** Correspondence:**
Dr Emily L. Clark
Emily.Clark@roslin.ed.ac.uk
Dr Mazdak Salavati
Mazdak.Salavati@roslin.ed.ac.uk

Keywords: Allele-specific expression, mapping bias, RNA-Seq, sheep, transcriptome, WASP, GeneiASE
Running title: Unbiased ovine allele-specific expression
Editorial choice: British English
Article type: Original Research
Manuscript length: 6361 words

Abstract

Pervasive allelic variation at both gene and single nucleotide level (SNV) between individuals is commonly associated with complex traits in humans and animals. Allele-specific expression (ASE) analysis, using RNA-Seq, can provide a detailed annotation of allelic imbalance and infer the existence of cis-acting transcriptional regulation. However, variant detection in RNA-Seq data is compromised by biased mapping of reads to the reference DNA sequence. In this manuscript we describe an unbiased standardised computational pipeline for allele-specific expression analysis using RNA-Seq data, which we have adapted and developed using tools available under open licence. The analysis pipeline we present is designed to minimise reference bias while providing accurate profiling of allele-specific expression across tissues and cell types. Using this methodology, we were able to profile pervasive allelic imbalance across tissues and cell types, at both the gene and SNV level, in Texel x Scottish Blackface sheep, using the sheep gene expression atlas dataset. ASE profiles were pervasive in each sheep and across all tissue types investigated. However, ASE profiles shared across tissues were limited and instead they tended to be highly tissue-specific. These tissue-specific ASE profiles may underlie the expression of economically important traits and could be utilized as weighted SNVs, for example, to improve the accuracy of genomic selection in breeding programmes for sheep. An additional benefit of the pipeline is that it does not require parental genotypes and can therefore be applied to other RNA-Seq datasets for livestock, including those available on the Functional Annotation of Animal Genomes (FAANG) data portal. This study is the first global characterisation of moderate to extreme ASE in tissues and cell types from sheep. We have applied a robust methodology for ASE profiling, to provide both a novel analysis of the multi-dimensional sheep gene expression atlas dataset, and a foundation for identifying the regulatory and expressed elements of the genome that are driving complex traits in livestock.

Introduction

Allele-specific expression (ASE) is the imbalance of allelic expression between parental (diploid) copies at the same locus (Barlow and Bartolomei, 2014). It is most commonly associated with cis-acting regulatory variation that may mediate parent-of-origin, sex- or tissue-specific transcription of one allele relative to the other (Renfree et al., 2009; Hasin-Brumshtein et al., 2014). In a single individual, where there are informative sequence variants (i.e. heterozygote loci) that distinguish the products of two alleles, ASE can be detected by RNA-sequencing (Chamberlain et al., 2015; GTEx Consortium et al., 2017; Cao et al., 2019; Guillocheau et al., 2019). The ratio of allelic read counts obtained from RNA-Seq datasets can be used as a reliable proxy for ASE (i.e. $ASEratio = CountsAllele1/(CountsAllele1 + CountsAllele2)$) (Edsgärd et al., 2016).

Large and complex RNA-Seq datasets give rise to unique and interesting computational challenges, in particular the elimination of reference mapping bias in ASE analysis of diploid genomes. RNA-Seq data are commonly mapped against reference genomes which are typically 'flat', with each position represented only by the reference (most abundant) allele. As such, reads containing heterozygous loci are more likely to be erroneously mapped (Degner et al., 2009; Stevenson et al., 2013; Hodgkinson et al., 2016). This can lead to high false positive ASE locus discovery rates (Degner et al., 2009). Although development of de novo transcript assemblers (Zerbino and Birney, 2008), variant-aware aligners (Xin et al., 2013; Hach et al., 2014) and mapping-free quantification e.g. Kallisto ((Bray et al., 2016)) has removed some of the issues, reference allele mapping bias remains an unresolved challenge in ASE studies. The analysis pipeline we present in the manuscript is designed to minimise reference bias while providing accurate profiling of allele-specific expression in large and complex RNA-Seq datasets.

We have developed an ASE analysis pipeline using the combination of software available under open licence, WASP (reference mapping bias removal) (van de Geijn et al., 2015), GATK (ASEReadCounter) (McKenna et al., 2010; Van der Auwera et al., 2013) and GeneiASE (Liptak-Stouffer aggregative ASE gene model) (Edsgärd et al., 2016). The GeneiASE model is capable of testing ASE at the gene level using two approaches: i) Static ASE which measures allelic imbalance within a gene (i.e. when ASE variants are located within the boundaries of the gene) and ii) Individual condition dependent ASE (ICD) which measures inducible ASE in a gene under an environmental pressure between 2 timepoints (i.e. in stimulated or unstimulated immune cells).

In addition to ASE at the gene level, we can also measure significant ASE at the single nucleotide level (SNV). ASE has been shown to be enriched within expression quantitative trait loci (eQTL) regions (Montgomery et al., 2010), therefore identifying ASE variants can be useful for understanding the transcriptomic control of complex traits in livestock. Complex trait mapping of ASE loci has been associated with phenotypes such as resistance to Marek's disease in chicken (Meydan et al., 2011) and pigmentation patterns in sheep (García-Gámez et al., 2011).

Understanding ASE is also important because cross-breeding now underlies most livestock production systems. Knowledge of ASE may provide insights into the molecular basis of the complex phenomenon of hybrid vigour, as emphasised by recent studies on two Chinese goat breeds and their F1 hybrids (Cao et al., 2019) and in F1 crosses of two highly inbred chicken lines (Zhuo et al., 2017). In this study we measure ASE in cross-bred sheep. Sheep are an economically important livestock species in many countries across the globe and particularly in emerging economies. The identification of prevalent ASE in populations or breeds, especially in economically relevant phenotypes and tissues, could be used to improve genomic prediction in sheep breeding programmes, such as those that have been established in

Australia and New Zealand (Daetwyler et al., 2010).

Using the methodology we describe, for mapping bias correction and robust positive ASE discovery, we were able to profile pervasive allelic imbalance across tissues and cell types, at both the gene and SNV level, in Texel x Scottish Blackface sheep. We analysed a subset of total RNA-Seq libraries from liver, spleen, ileum, thymus and bone marrow-derived macrophages (BMDM) (+/-) lipopolysaccharide (LPS), from six individual adult cross-bred sheep to produce a detailed picture of allelic imbalance in immune-related tissues and cell types. We chose to focus this analysis on immune related tissues in part because of the depth of available sequence in those tissues, and in part because they contain abundant immune cell populations. The diversity of cell populations is reflected in the transcriptional complexity of immune tissues and cell types in the sheep gene expression atlas dataset (Clark et al., 2017; Bush et al., 2018). As such this subset of tissues gave us a transcriptionally rich dataset in which to measure ASE. We also included BMDMs stimulated and unstimulated with LPS to mimic infection with Gram-negative bacteria, in order to test whether ASE changed in response to stimulation with LPS in these cells. By measuring ASE in these tissues and cell types from sheep we were able to: i) provide insight into how pervasive ASE is across tissues at the gene and SNV level, ii) generate tissue-specific ASE profiles, iii) investigate sex-specific patterns of ASE, and iv) determine the extent to which ASE changes in response to stimulation with LPS in an immune cell type. This novel analysis of the multi-dimensional sheep gene expression atlas dataset provides a foundation for further analysis of the regulatory and expressed elements of the genome that are driving complex traits in sheep.

Methods

Sample preparation and RNA extraction

Data from three male and three female Texel x Scottish Blackface (TxBF) sheep from the sheep gene expression atlas project (Clark et al., 2017) were used in this study. The dataset including: 2 cell types (BMDMs (+/-) LPS) and 4 tissues (thymus, spleen, liver and ileum). Tissue collection, storage and RNA extraction is described in (Clark et al., 2017). BMDM's were cultured in vitro for 7 days in the presence of macrophage colony-stimulating factor (CSF1 (10^4 U/ml) and unstimulated (0 hrs - LPS) and stimulated (7hrs +100ng/ml LPS) samples of BMDMs were obtained also as described in (Clark et al., 2017). A total of 2 samples (1 thymus and 1 spleen) did not pass the RNA quality control (RNA integrity number (Mueller et al., 2004); RIN <7) and were not included in the sheep gene expression atlas. Library preparation was performed by Edinburgh Genomics (Edinburgh Genomics, Edinburgh, UK). All total RNA Illumina TruSeq libraries (125bp paired end) were sequenced at a depth of > 100 million reads per sample.

Reference mapping bias removal

BAM files from RNA-Seq data, were previously mapped to Oar v3.1 top level DNA fasta track, using HISAT2 as described in (Clark et al., 2017). These BAM files were used to locate reads with heterozygote loci using WASP's find_intersecting.py script (van de Geijn et al., 2015). The intersection of reads and heterozygote loci in all samples were based on the Ensembl v92 variant call format (VCF) track (Ensembl v92: ovis_aries_incl_consequences.vcf.gz). Synthetic copies of reads containing heterozygote loci, were created with the alternate allele flipped to the remaining options of A, T, C or G (up to 6 loci /read[2^n] max 64 combinations of synthetic reads) using parameters defined in WASP (van de Geijn et al., 2015). This was followed by remapping of the synthetic reads using HISAT2

(Li and Durbin, 2009; Kim et al., 2015) and eliminating the original reads (and their synthetic copies) which mapped to a different coordinate in any of its synthetic copies (WASP's filter_reads.py) (van de Geijn et al., 2015). After merging the retained reads with non-intersecting reads, a final BAM file was produced for ASE read counting step (WASP's remove_dup.py).

Allelic read counts and depth filtration

Allele-specific read counting was carried out using the ASEReadCounter module of GATK v3.8 with parameters -mmq 50 -mbq 25 (McKenna et al., 2010). Multiple pre-processing steps were performed prior to GeneiASE input as instructed by (Edsgärd et al., 2016) which included, preparing per chromosome indices, merging the variant set with corresponding gene coordinates and bi-allelic expression filtering. Loci with < 10 reads mapped were excluded, as were loci with < 3 reads, or < 1% of the total reads, mapped to both the reference and alternative allele. This form of filtration will eliminate loci exhibiting mono-allelic expression (MAE) as previously described (Degner et al., 2009; Stevenson et al., 2013; Mayba et al., 2014). Similar filtration criteria have been previously used routinely in ASE studies (Mayba et al., 2014; Chen et al., 2016a; Edsgärd et al., 2016; GTEx Consortium et al., 2017; Raghupathy et al., 2018; Cao et al., 2019; Guillocheau et al., 2019; Gutierrez-Arcelus et al., 2019).The workflow of the analysis pipeline for ASE analysis is detailed in Fig.1.

Experimental design for defining allele-specific expression

ASE was defined according to the following three categories:

i) Static ASE: which is inherent allelic imbalance (AI) in each gene calculated by ASE at all heterozygote loci (i.e. $ASE = Counts\ RefAllele/(Counts\ RefAllele + Counts\ AltAllele)$ within the boundaries of the gene. The effect size of ASE at gene level was produced by aggregation of the ASE effect size at SNVs within the gene boundaries (the Liptak-Stouffer method, applied by the GeneiASE aggregative model). A null distribution of ASE effect size for genes in each transcriptome was produced by random sub-sampling (n = 1e+5) from a pool of genes having min 2 and max 100 loci within their boundaries. The ASE effect size of each gene (aggregated using Liptak-Stouffer) was then tested against the null distribution of same SNV number, via a modified bi-nomial test (2x1 table). Distribution of p values was examined for uniformity prior to false discovery rate correction (Supplementary file1) (Benjamini and Hochberg, 1995; Pounds and Cheng, 2006; Barton et al., 2013).

ii) Individual condition-dependent ASE (ICD-ASE): in which the same ASE effect size was calculated for each gene in the treated versus the untreated timepoints of the same sample (i.e. BMDM +/- LPS). The log2ratio ($ASE_{treated}/ASE_{untreated}$) was used in a beta-binomial test (2x2 table) similar to the static mode. The details of this aggregative model have been previously described in the GeneiASE publication (Edsgärd et al., 2016).

iii) Condition dependent ASE at SNV level: in which a contingency table was produced for read counts (ref and alt) for every SNV, present both in treated and untreated conditions (BMDM +/- LPS) (2x2 table) and a Fisher's exact test performed followed by p value multiple testing correction (Benjamini and Hochberg, 1995). The p values from loci showing ASE and shared by the six adult sheep (ID and coordinate) were unified, using the Stouffer method

(Dewey, 2016, 2018) and presented as false discovery rate (FDR) for each locus.

Static ASE was calculated in both tissues and BMDMs (each timepoint was considered separately for BMDMs). Condition dependent ASE analysis was carried out only in BMDMs ± LPS both at gene (ICD-ASE) and SNV (Fisher's exact) level to study LPS inducible ASE.

Statistical analysis and thresholds applied

The extraction, transformation and loading of the all datasets and subsequent statistical analysis was carried out in R v ≥ 3.4 unless stated otherwise (R Core Team, 2017). System query language join statements (Wickham and Francois, 2015) were used to compare lists of ASE genes or SNVs between samples. Raw p values resulting from all three types of ASE analysis were corrected for multiple testing via Benjamini-Hochberg false discovery rate calculations (Benjamini and Hochberg, 1995). The passing threshold of significance in all analyses was considered to be FDR < 0.1 (10%) except for the Fisher's exact test association study. Genes showing ASE in multiple tissues were considered those for which 4 or more of the 6 sheep had significant ASE.

Results

Estimation of heterozygous sites across all individuals

To determine the level of heterozygosity present in the RNA-Seq data we first assessed the number of bi-allelic heterozygote sites per individual for each of the six sheep (range= 5,673,703-6,438,497) detailed in Fig.2. Individual variation was observed in the SNVs per gene in each sheep (Fig.2A&C). However, there was no significant difference in the total number of bi-allelic SNVs captured in the RNA-Seq data across all six individuals or between the male and female sheep included in the study (Fig.2B). The bi-allelic SNVs captured in the RNA-Seq data set were annotated using the Ensembl v.92 (Zerbino et al., 2018) reference VCF track. The distribution of SNVs per gene in the Ensembl track is tail-inflated in comparison to the RNA-Seq data Fig.2A. This issue could be due to erroneous assignment of SNVs in hypervariable and repetitive regions, multi-allelic SNVs or simply that there are variants in the Ensembl track that are not expressed (transcribed). The distribution of SNVs for each individual is shown in Fig.2C.

Reference mapping bias elimination and quality control

We used the WASP ref bias removal script to successfully minimise ref allele mapping bias in the RNA-Seq samples. The mapping bias was assessed by global distribution of the allelic ratio i.e. $ref_{counts}/alt_{counts} + ref_{counts}$ in each RNA-Seq sample as shown in Fig.3. The ASE discovery rate at the SNV level on average constituted 5.8% of the heterozygote loci that passed the minimum filtration criteria in each individual (0.1% of the total expressed). This portion of the transcriptomic variants belonged to an average of 103 genes in each tissue transcriptome (approx.1%) or 300 in each individual (Supplementary file4 – S4 Fig.1 and Fig.2). As shown in S4 Fig 2. expression level varies across tissues but this does not affect the distribution of ASE genes.

Genes exhibiting tissue-specific and pervasive ASE signatures

We used the static mode of GeneiASE to investigate pervasive and tissue-specific ASE

profiles across all of the available samples. The number of genes showing significant static ASE in immune-related tissues across the six sheep are summarised in Table 1. On average approximately.0.5% of the genes in each tissue-specific transcriptome showed significant ASE (approx. 1% of the filtered set of genes). Pervasive ASE genes in all 4 tissues for each of the 6 sheep was investigated by applying the minimum 67% shared rule (i.e. min 4 out of 6 sheep shared significant ASE for the gene). Genes exhibiting significant ASE shared by all 4 tissues were then merged and the ASE effect size averaged (Fig.4A). Six genes exhibited pervasive ASE across tissues (i.e. they were shared across all 4 tissues). In the order of allelic imbalance effect size they were NAA50 (N(alpha)-acetyltransferase 50, Histone acetyl transferase) with highest ASE effect size in spleen, UBB (Ubiquitin B, protein degradation) in thymus, HBP1 (HMG-Box transcription repressor; cell cycle regulation) and ENSOARG00000016510 both in spleen, C1orf105 (Chromosome 1 Open Reading Frame 105) in ileum and MTIF2 (mitochondrial translational initiation factor 2) in thymus.

Sets of genes with tissue-specific ASE profiles were also captured (Fig.4B-E). Thymus had the highest number of tissue-specific ASE genes (n=15) followed by liver (n=12), spleen (n=5) and ileum (n=4) (Fig.4B-E). Amongst the thymus gene set was CD244 which included 30 heterozygote loci with allelic imbalance, one of which was rs406633825. This missense allele (Chr1:110308273 C>A; pVal123Phe MAF=0.7, SIFT score=0 deleterious) has previously been reported in the Texel population characterised by the International Sheep Genome Consortium (ISGC) (Kijas et al., 2012). The liver-specific ASE profile included genes involved in amino acid metabolism, cytochrome oxidase pathways and fibrinogen: FGA (fibrinogen alpha chain), ENSOARG00000003175 (taurochenodeoxycholic 6 alpha-hydroxylase-like, cytochrome P450 family 4 member [CYP4]), ENSOARG00000001568 (novel gene, complement C4-A-like), CYP3A24 (cytochrome P450 family 3 member) and CA3 (carbonic anhydrase 3). Allelic imbalance in spleen was present in CACYBP (calcyclin binding protein), DAPK2 (death associated protein kinase [serine/threonine]) and a novel gene GIMAP8-like (ENSOARG0000001131). The ASE in GIMAP8 has been previously reported in cattle with a strong paternal parent-of-origin expression pattern (Chamberlain et al., 2015). The GIMAP/IAN family of proteins, which are involved in survival, selection and homeostasis of lymphocytes (Nitta and Takahama, 2007).

Two genes of functional interest showed evidence of strong tissue-specific ASE in the spleen: SNAP23 and MYLK. SNAP23 is a key molecule in vesicle transport machinery of the cell and has been reported to be expressed in sheep spleen. SNAP23 or Synaptosome Associated Protein 23 is part of protein complex involved in Class 1 MHC mediated antigen processing and presentation and in neutrophil degranulation (Fabregat et al., 2018). SNAP23 is also vital to lymphocyte development (both B and T) in vitro (Wong et al., 1997; Kaul et al., 2015). The myosin light chain kinase (MYLK) expression in the splenic trabeculae's smooth muscle has been demonstrated previously (Jiang et al., 2014; Clark et al., 2017). Overall 199 heterozygote bi-allelic loci were present within the MYLK gene. The variant rs400678033 (Chr1:186347056G>A; .pAla1014Val), a missense SNV in exon 17 of 33 exons in MYLK, showed consistent allelic imbalance in all spleen samples.

In summary, analysis of ASE across immune related tissues revealed there were a small number of genes that were shared across tissues. ASE signatures instead tended to be tissue-specific, within the sub-set of tissues investigated in this study.

Individual-specific ASE signatures

In order to investigate whether ASE profiles were either shared across all six sheep or private to individual sheep we used intersectionality (Fig.5). Each tissue was investigated separately. A number of private (to each individual) ASE genes were detected for each tissue,

ranging from: 31-123 in ileum (Fig.5A), 24-80 in liver (Fig.5B), 21-83 in spleen (Fig.5C) and 31-66 in thymus (Fig.5D). Some of the shared sets of ASE genes in these tissues were specific to either male or female sheep, these sex-specific ASE signatures are described in Fig.5. In ileum no sex-specific set was observed (Fig5A). In contrast to ileum, the ASE profile for liver included a single gene with female only membership, ENSOARG00000017409 (novel gene; 93% orthology with bovine dicarbonyl and L-xylulose reductase [DCXR]) Fig.5B. In spleen all female sheep shared significant ASE in PMS1 (DNA mismatch repair system component during post meiotic segregation), ANKRD10 (Ankyrin Repeat Domain 10) and ENSOARG00000006103 which was not present in any of the spleen profiles of male sheep (Fig.5C). In thymus there were 2 sex-specific sets: 16 genes showing ASE only in females and 5 genes only in males. The female-specific thymus gene set included: ARPP21 (cAMP regulated phosphoprotein 21), CDKL3 (cyclin dependent kinase like 3), CEP19, ENSOARG00000000710 (novel gene), ENSOARG00000001163 (novel gene), ENSOARG00000000710, ENSOARG00000001163, ENSOARG00000008981 (novel gene; T-lymphocyte surface antigen Ly-9-like), ENSOARG00000006215, ENA000000008981, ENSOARG00000009129, ENSOARG00000011375 (blood vessel epicardial substance [BVES]), ENSOARG00000015755, ENSOARG00000020354 (novel gene; 53% orthology with bovine monoacylglycerol acyltransferase [MOGAT1]), ENSOARG00000025005, ENSOARG00000026030 (novel gene), GPM6A (glycoprotein M6A), RAG1 (recombination Activating 1), STX8 (syntaxin 8). The male-specific thymus set was comprised of ENSOARG00000007267 (novel gene; T-cell surface glycoprotein CD1a-like), ENSOARG00000016841 (novel gene; 98% orthology with bovine ATP synthase membrane subunit G [ATP5MG]), ENSOARG00000007603, SNX25 (sorting nexin 25) and LDHA (lactate dehydrogenase A) Fig.5D.

In summary very few ASE genes were shared across all sheep and the majority of ASE profiles were private to each sheep. Sex-specific ASE signatures were also detected but due to the small sample size (n=3) in both cases these should be interpreted with caution.

ASE in stimulated and unstimulated BMDMs (0hrs vs 7hrs +LPS)

We examined inducible ASE after 7 hrs of exposure to LPS in BMDMs using the ICD mode of GeneiASE (Edsgärd et al., 2016). A comparison of LPS inducible ICD-ASE genes and the genes with background static ASE at 0 and 7 hr time points, was also performed. We first assessed whether differences between 0 and 7 hours could be observed using analysis of static ASE. Individual-specific ASE profiles and a limited number of shared ASE genes were also observed in BMDMs. The total number of genes with static ASE in the BMDMs is shown in Table 2.

Shared static ASE across both time points and independent of LPS induction was only observed in 5 genes. These genes have a macrophage associated function and include ITGB2 (Yee and Hamerman, 2013), SAA3 (ENSOARG00000009963) (Larson et al., 2003; Deguchi et al., 2013), CD200R1 (ENSOARG00000019357) (Ocaña-Guzman et al., 2018), DCTN5 (ENSOARG00000017281) (Habermann et al., 2001) and MTIF2 (also seen in the tissue analysis above) (Overman et al., 2003).

The ICD-ASE in BMDMs +/-LPS captured fewer ASE genes with significant LPS inducible ASE between the 2 timepoints than the static analysis of ASE. Moreover, there were large differences in the number of LPS inducible ASE in each individual sheep, indicating significant individual-specific variation in response to LPS stimulation. BMDM cultured from female 2 showed no LPS inducible response in comparison to male 3 which was a hyper responder with significant inducible ICD-ASE in 28 genes (including 634 informative SNVs total). A detailed breakdown of SNVs, aggregated within each gene, with significant ICD ASE

has been summarised in Fig.6.

In summary the ICD-ASE mode of GeneiASE's model was not capable of capturing a complete picture of differential ASE in the BMDM experiment. Static ASE was present in both time points, however, there were no inducible ASE genes that were shared across all 6 sheep. The highly diverse ASE profile of BMDMs was very individual-specific, similar to patterns observed in tissues (Supplementary file4. S4 Table 1). These individual-specific differences could be due to individual variation in the innate immune response or experimental variation introduced during primary cell culture or stimulation with LPS.

Condition dependent ASE at the SNV level in BMDMs

To further investigate allelic imbalance at the SNV level without the aggregative gene model of GeneiASE, Fisher's exact test was used. The filtered read counts for bi-allelic SNVs shared by all 6 sheep BMDMs were selected (n=646 sites). Allelic read counts of each SNV were tested using Fisher's exact test between 0hrs and 7hrs (2x2 table). Overall the 6 sheep shared 646 SNVs with identical allelic genotypes in both time-points of the BMDM RNA-Seq dataset. These SNVs were tested for association with LPS treatment and only 4 SNVs showed a strong association (FDR < 1.0e-8) and 12 SNVs had an FDR between 1.0e-02 and 1.0e-08 (Fig.7). The highest F-statistic was at rs430667535Chr17 Pos:50485358T>C, a synonymous variant in ubiquitin C (UBC), a polyubiquitin precursor, and also an intronic variant T>C or A>G in pro-apoptotic BRI3 binding protein (BRI3BP). This variant was shown to have a minor allele frequency (MAF) of 0.25 in Texel sheep based on the ISCG annotation [ISGC – Ensembl v.92](Kijas et al., 2012)). The next highest peak was observed on Chr21 under SNVs within SAA3 gene boundaries (ENSOARG00000009963) at the following coordinates: Highest FDR peak was observed at SNV rs412192652 (Pos:25826978A>G missense variant [Asn145Asp], FDR=2.3e-15) surrounded by rs403064928 (Pos:25826884C>A missense variant [Asp113Glu] in exon 4 of SAA3 FDR=3.6e-07), rs426609498 (Pos:25826845A>G synonymous, FDR=5.5e-07) and rs405439099 (Pos:25826990G>C 3'UTR variant, MAF 0.6 in Texel sheep, FDR=4.1e-05). This region contains a strong LD block previously reported by the ISGC COMPOSITE population (Ensembl v.92) (Supplementary file3) e.g. rs412192652 and rs405439099 pairwise D' statistics = 1. Two further peaks on Chr3 were observed for rs159926581 (Pos:214731375T>C synonymous, FDR = 3.3e-09) in ribosomal protein L3 (ENSOARG00000016495) and rs159822214 (Pos:112164732G>A 3'UTR variant, FDR=9.5e-03) in oxysterol binding protein like 8 (OSBPL8). The last inducible ASE associated signal was on Chr16 rs420037698 (Pos:6887423G >A, FDR= 6.9E-09) in ENSOARG00000004700, a known synonymous variant in the Texel population (MAF = 0.55). The SNVs and corresponding genes from Fisher's exact test are summarized in Table 3.

The LPS inducible ASE analysis, of SNVs, using Fisher's exact test revealed a different picture not captured by the gene level analysis with the GeneiASE model that aggregates SNVs within each gene (Fig.6 vs Fig7). The aggregative gene model did not capture any shared ASE genes in the ICD-ASE mode. Although the 6 sheep shared 646 SNVs and showed highly significant association with stimulation with the LPS (Fisher's exact method), the aggregation of ASE effect size from SNV to gene level (ICD-ASE mode) only detected individual-specific sets of ASE genes in each sheep. This contradicted the results from Fisher's exact test which detected 4 highly significant LPS inducible shared regions (FDR < 0.01, 16 SNVs) on chromosomes 3, 16, 17 and 21. For example, the allelic imbalance in the SAA3 genomic coordinates on chromosome 21 was not detectable in the ICD-ASE model but it was captured by the Fisher's exact test in all individuals (Fig.7B chromosome 21).

Fisher's exact analysis at SNV level revealed ASE in response to LPS in variants within CLDN1, ANXA3, BRI3BP, SAA3 and MSR1 (Table3). The anti-inflammatory macrophage

marker CLDN1 (Van den Bossche et al., 2012) and acute-phase inflammation resolution marker ANXA3 (Yamanegi et al., 2018) have been previously reported with distinct macrophage functions. The macrophage scavenger receptor 1 (MSR1) has also been shown to be involved in lipid uptake and migration ability of macrophages (Shi et al., 2019). Three noncoding RNAs (RF00221 [snoRD43], RF00593[snoU83B] and RF01151[snoU82P] were amongst genes corresponding to ASE inducible SNVs. These 3 snoRNAs all overlap with the genomic coordinates of ribosomal protein L3 (ENSOARG00000016495 / RPL3). The RF00377 [snoU6-53] was also among the ASE positive targets which overlaps the protein-coding gene CDS2 (CDP-diacylglycerol synthase 2). Using bulk RNA-Seq makes it difficult to differentiate the origin of the ASE signal to specific RNA populations.

In summary ASE profiles in BMDMs were highly individual-specific at both gene and SNV level. Moreover, Fisher's exact SNV level analysis discovered shared ASE SNVs where the aggregative gene model of ICD-ASE mode did not, indicating for condition dependant ASE analysis Fisher's exact test is more accurate and robust at SNV level.

Discussion

This study is the first to investigate global allele-specific expression across tissues from sheep using RNA-Seq data. We focused our analysis on immune-related tissues and cell types from six adult cross-bred sheep (TxBF) from the sheep gene expression atlas. ASE profiles were highly individual-specific in the six sheep analysed in this study. We were able to identify tissue-specific sets of ASE genes, as well as LPS inducible sets in the BMDM experiment. Tissue-specific signatures of ASE have been previously reported in similar studies in mouse (Castel et al., 2015, 2016), goat (Cao et al., 2019) and cattle (Chamberlain et al., 2015).

Several steps were taken in the cattle study (Chamberlain et al., 2015) to mitigate the ref allele bias, assign parental origin using whole genome sequences and include MAE variants. The SNV filtration was based on the (Hayes and Daetwyler, 2019) 1000 bull genomes project to confirm the heterozygote sites. In our pipeline the Ensembl VCF track was used for that purpose. In the cattle study the 1 and 0 inflated ref allelic ratio was still present and the ASE analysis was done via introduction of 0.9 allelic ratio cut-off. In our pipeline no cut-off is introduced and because it is difficult to distinguish between sequencing error and MAE, a minimum filtration criteria was applied to exclude MAE. Chamberlain et al. tested 5317 genes (14,495 SNVs) in spleen and detected 382 ASE genes (with min > 1 SNV per gene, similar to this study). Although direct comparison would not be appropriate (because we have excluded MAE variants in our analysis) our analysis of sheep spleen revealed ASE in 86 genes (average in 5 sheep) from 8272 filtered genes (average in 5 sheep). Similarly, in thymus the cattle study showed 182 ASE genes from 986 informative genes (9781 SNVs) while from 7961 filtered genes in sheep thymus 134 ASE genes were captured. The differences in the numbers of genes exhibiting ASE between the two studies are likely to be a consequence of the filtration criteria applied, the exclusion of MAE, and species-specific differences between sheep and cow. Results from a more recent study in goat (Cao et al., 2019) more closely reflect our findings. They apply similar filtration criteria to our workflow and discovered 144 ASE genes in liver in comparison to 123 in our sheep liver sets (averaged across 6 sheep). Other recent studies including those focusing on production relevant tissues, such as muscle (Guillocheau et al., 2019), have also applied similar stringency in filtration criteria. The filtering criteria we have used for this analysis is stringent and focused on detecting variants of moderate to extreme effects. Further analysis of the dataset reducing these criteria might discover additional variants exhibiting ASE across individuals and tissues, but it would also increase the potential risk of false positive discovery.

For this analysis we have adapted an ASE analysis workflow with a primary focus on

mapping bias removal prior to allele-specific analysis of the transcriptome. The collection of scripts for WASP, used for this analysis, or modified versions of them have been utilised by others for mapping bias removal in reference guided genomic datasets e.g. RNA-Seq (Mozaffari et al., 2018; Zhou et al., 2018), Chip-Seq (Pelikan et al., 2018) and for methylomic and epigenetic analysis (Richard Albert et al., 2018).

The ASE analysis pipeline we have adapted for sheep for this study is also adaptable to other species and tissue types with available RNA-Seq datasets. It could be applied, for example, to profile allele-specific expression in the RNA-Seq datasets from livestock species listed on the FAANG data portal (Andersson et al., 2015; Harrison et al., 2018). We used the Ensembl VCF track to capture information at heterozygote loci however the individual VCF file from each sheep could also be used in ASE analysis. The latter strategy might enable the capture of rare variants not included in the publicly available VCF tracks but would also raise the issue of normalisation/standardization between VCF call sets. The usage of either of these methods will be limited to the number of loci shared by coordinate and bi-allelic genotype (i.e. pervasive ASE discovery). Other studies have compared variants at the RNA and DNA level from the same individual and then removed the DNA variants not present in the RNA-Seq data from the analysis (Guillocheau et al., 2019). We believe that a strength of the pipeline we present is that it does not require parental genotypes and can therefore be applied to other RNA-Seq datasets for livestock where this information is not available.

In our analysis we have not considered either parent-of-origin or breed-of-origin-specific effects in this analysis. For parent-of-origin or breed-of-origin assignment of these ASE profiles DNA level genotypes from the parents of the six sheep from the gene expression atlas (i.e. Texel sire and Scottish Blackface dam) would be required, and these are unfortunately not available. In this study ASE expression profiles also might be affected by the direction of the cross (i.e. Texel sire x Scottish Blackface dam). To fully characterise parent-of-origin or breed-of-origin reciprocal cross experiments would be required. Reciprocal cross studies in mouse (Huang et al., 2017), chicken (Zhuo et al., 2017) and cross-bred cattle (Chen et al., 2016b) have shed light on the complexity of such pervasive ASE markers and parent-of-origin effects. Though potentially very interesting these experiments are lengthy and costly to perform in sheep. Particularly in this case because the reciprocal cross (Scottish Blackface dam x Texel sire) is rarely used in the UK sheep industry and as a consequence has limited relevance to production.

Our approach also excludes mono-allelic expression. The minimum filtration criteria utilised in our workflow along with the reference mapping bias removal step ensures an unbiased ASE discovery in the transcriptome by excluding the ambiguity surrounding MAE variants. This form of analysis is based on the principle that absence of evidence (reads) for either allele of a heterozygote site does not directly amount to evidence of their absence i.e. MAE. The pattern of ASE (ratio of Alt/Ref+Alt) is dependent on the bi-allelic expression of loci within the genomic coordinates of the gene or genomic element of interest. For an ASE effect to be captured by the GeneiASE model, the following criteria must be met: i) Biallelic expression of the locus; ii) Min depth criteria for each allele (min 3 reads , total 10 reads at that site and > 1% of total reads containing that allele); iii) The allelic imbalance or departure from bi-allelic balanced expression being inducible by an environmental trigger (i.e. LPS in ICD ASE experiment with BMDM data). These stringent criteria secure robust transcriptome-wide ASE discovery while maximising the usage of read counts from short read RNA-Seq datasets without considering mono-allelic sites. MAE patterns are impossible to differentiate from sequencing error or random nonsense mediated decay in bulk RNA-Seq, unless arbitrary cut-offs are introduced such as ratio of allelic read counts > 0.9 (Chamberlain et al., 2015) or > 0.7 (Cao et al., 2019). We decided to exclude MAE from this study for the aforementioned reasons.

The tissues utilised for ASE analysis in this study (thymus, spleen, liver and ileum) are

highly influential on performance of the immune system. ASE profiles shared across tissues and cell types were limited and instead they tended to be highly specific. We identified tissue-specific ASE in several genes in Thymus, for example, that are involved in the T-cell mediated immune response, including CD47 and CD244. These tissue-specific and cell-type-specific ASE profiles may underlie the expression of economically important traits such as disease resistance. Assessment of the connection between economically relevant phenotypes and tissue-specific ASE profiles could be useful for the improvement of genomics enabled sheep breeding programmes, particularly those using specialised sire and dam lines (Georges et al., 2018). Loci exhibiting ASE have been associated with production traits including milk-fat percentage (Hayes et al., 2010; Suárez-Vega et al., 2017), trypanotolerance in small ruminants (Kadarmideen et al., 2011; Álvarez et al., 2016), mastitis in goat (Ilie et al., 2018), Johne's disease in cattle (Mallikarjunappa et al., 2018) and Marek's disease in chicken (Maceachern et al., 2011; Meydan et al., 2011; Cheng et al., 2015). Although there is no general consensus currently on the correlation of allelic expression haplotypes and phenotypes under selection in sheep, this form of ASE analysis could pave the way for functional validation at population level (e.g. breed or haplotype-specific aseQTL studies in a larger population of sheep). Examples of population level aseQTL, eQTL and sQTL (QTLs associated with RNA splicing) already exist for cattle (Wang et al., 2018; Xiang et al., 2018). Knowledge of favourable ASE in critical genes involved in traits of interest could be used as a performance indicator or included as weighted SNVs in genomic prediction algorithms to enhance livestock breeding programmes (Georges et al., 2018). Currently the UK sheep industry is on the cusp of applying genomic prediction, but suitable genomics enabled breeding programmes for sheep already exist in New Zealand and Australia (Daetwyler et al., 2010).

Conclusions

In this study we characterise extreme to moderate allele-specific expression, at the gene and SNV level, in immune-related tissues and cells from six adult sheep (TxBF) from the sheep gene expression atlas dataset. Reference mapping bias removal was an integral component of the analysis pipeline applied in this study. The correction of reference bias prior to obtaining the allelic read counts is a critical step toward true ASE discovery. The workflow developed as part of this manuscript provides an RNA-Seq only dependent tool, without the need for individual DNA sequences. We note that the stringent filtering process applied would remove loci where the allelic imbalance was less extreme but might still be of biological significance.

This study is a novel analysis of an existing large-scale complex RNA-Seq dataset from sheep. Using the pipeline we have adapted for this analysis, we were able to identify ASE profiles that were pervasive in each sheep and specific to the tissues and cell types investigated. These tissue and cell-type-specific ASE profiles may underlie the expression of economically important traits and could be used to identify variants that could be weight in genomic prediction algorithms for the improvement of sheep breeding programmes. In summary we have adapted a robust methodology for ASE profiling, using the sheep gene expression atlas dataset, and provided a foundation for identifying the regulatory and expressed elements of the genome that are driving complex traits in livestock.

Data Availability

The RNA-Seq sequence data is available via the European Nucleotide Archive (ENA) under PRJEB19199 (https://www.ebi.ac.uk/ena/data/view/PRJEB19199). The BAM files were already produced as part of the sheep gene expression atlas following the publicly available protocol (FAANG, 2018) and as described in (Clark et al. 2017). The BAM files have been

uploaded to ENA under accession numbers ERZ827944, ERZ827949, ERZ827951, ERZ827955, ERZ827972, ERZ827988, ERZ827995, ERZ827997, ERZ828001, ERZ828016, ERZ828019, ERZ828036, ERZ828044, ERZ828046, ERZ828050, ERZ828070, ERZ828073, ERZ828160, ERZ828167, ERZ828168, ERZ828172, ERZ828188, ERZ828192, ERZ828209, ERZ828215, ERZ828217, ERZ828221, ERZ828240, ERZ828244, ERZ828261, ERZ828268, ERZ828270, ERZ828274, ERZ828293 and ERZ828297. The Oar v3.1 reference FASTA and VCF file from Ensembl v92 were used throughout the pipeline. The ASE analysis pipeline (https://msalavat@bitbucket.org/msalavat/asewrap_public.git) was wrapped using bash scripting on Edinburgh Compute and Data Facility computing resource Eddie Mark 3 (Edinburgh, 2018).

Author's contributions

MS and ELC coordinated and designed the analysis component of the study with assistance from SJB and SPV. MS and SPV designed, optimised and tested the ASE pipeline. DAH acquired the funding for the sheep gene expression atlas project. MEBM, ELC and DAH designed the LPS experiment and generated the data. MEBM performed the LPS stimulation of bone marrow derived macrophages and RNA extraction. SJB performed all bioinformatic analyses prior to analysis with the ASE pipeline. MS performed ASE analysis, visualisation of the results and wrote the manuscript. ELC contributed to manuscript editing and drafting. All authors read and approved the final manuscript.

Acknowledgments

The authors would like to thank University of Edinburgh Computing and Data Support staff (viz. Dr Andy Law and Dr Steve Thorn) for their input towards optimisation of the pipeline and efficient parallel computing. Rachel Young and Lucas Lefevre isolated the bone marrow derived macrophages for the sheep gene expression atlas project and Iseabail Farquhar helped to collect and archive the tissue samples. The authors would also like to thank Professor Kim Summers and Professor Mick Watson for their comments, which helped to improve the manuscript.

Conflict of Interest

The authors have no competing interest regarding the findings presented in this publication.

Funding

The work was supported by a Biotechnology and Biological Sciences Research Council (BBSRC) (http://www.bbsrc.ac.uk) Grant BB/L001209/1 ('Functional Annotation of the Sheep Genome'). Also, BBSRC Institute Strategic Program Grants: 'Farm Animal Genomics' (BBS/E/D/20211550), 'Transcriptomes, Networks and Systems' (BBS/E/D/20211552) and 'Blue Prints for Healthy Animals' (BB/P013732/1). Edinburgh Genomics is partly supported through core grants from BBSRC (BB/J004243/1), NERC (http://www.nerc.ac.uk) (R8/H10/56) and the Medical Research Council (MRC) (https://www.mrc.ac.uk) (MR/K001744/1). SJB was supported by the Roslin Foundation. ELC is supported by the University of Edinburgh Chancellor's Fellowship programme. The funders had no role in the study design, data collection and analysis, decision to publish, or preparation of the manuscript.

References

Álvarez, I., Pérez-Pardal, L., Traoré, A., Fernández, I., and Goyache, F. (2016). Lack of specific alleles for the bovine chemokine (C-X-C) receptor type 4 (CXCR4) gene in West African cattle questions its role as a candidate for trypanotolerance. *Infect. Genet. Evol.* 42, 30–3. doi:10.1016/j.meegid.2016.04.029.

Andersson, L., Archibald, A. L., Bottema, C. D., Brauning, R., Burgess, S. C., Burt, D. W., et al. (2015). Coordinated international action to accelerate genome-to-phenome with FAANG, the Functional Annotation of Animal Genomes project. *Genome Biol.* doi:10.1186/s13059-015-0622-4.

Barlow, D. P., and Bartolomei, M. S. (2014). Genomic imprinting in mammals. *Cold Spring Harb. Perspect. Biol.* 6. doi:10.1101/cshperspect.a018382.

Barton, S. J., Crozier, S. R., Lillycrop, K. A., Godfrey, K. M., and Inskip, H. M. (2013). Correction of unexpected distributions of P values from analysis of whole genome arrays by rectifying violation of statistical assumptions. doi:10.1186/1471-2164-14-161.

Benjamini, Y., and Hochberg, Y. (1995). Controlling the False Discovery Rate: A Practical and Powerful Approach to Multiple Testing on JSTOR. *Source J. R. Stat. Soc. Ser. B* 57, 289–300. Available at: https://www.jstor.org/stable/pdf/2346101.pdf?refreqid=excelsior%3A8080132077b9217878a58e47abbcf2d8 [Accessed October 27, 2015].

Bray, N. L., Pimentel, H., Melsted, P., and Pachter, L. (2016). Near-optimal probabilistic RNA-seq quantification. *Nat. Biotechnol.* 34, 525–527. doi:10.1038/nbt.3519.

Bush, S. J., McCulloch, M. E., Muriuki, C., Salavati, M., Davis, G. M., Farquhar, I. L., et al. (2018). Comprehensive transcriptional profiling of the gastrointestinal tract of ruminants from birth to adulthood reveals strong developmental stage specific gene expression. *bioRxiv*, 364752. doi:10.1101/364752.

Cao, Y., Xu, H., Li, R., Gao, S., Chen, N., Luo, J., et al. (2019). Genetic Basis of Phenotypic Differences Between Chinese Yunling Black Goats and Nubian Goats Revealed by Allele-Specific Expression in Their F1 Hybrids. *Front. Genet.* 10, 145. doi:10.3389/fgene.2019.00145.

Castel, S. E., Levy-Moonshine, A., Mohammadi, P., Banks, E., and Lappalainen, T. (2015). Tools and best practices for data processing in allelic expression analysis. *Genome Biol.* 16, 195. doi:10.1186/s13059-015-0762-6.

Castel, S. E., Mohammadi, P., Chung, W. K., Shen, Y., and Lappalainen, T. (2016). ARTICLE Rare variant phasing and haplotypic expression from RNA sequencing with phASER. *Nat. Commun.* 7. doi:10.1038/ncomms12817.

Chamberlain, A. J., Vander Jagt, C. J., Hayes, B. J., Khansefid, M., Marett, L. C., Millen, C. A., et al. (2015). Extensive variation between tissues in allele specific expression in an outbred mammal. *BMC Genomics* 16, 993. doi:10.1186/s12864-015-2174-0.

Chen, J., Rozowsky, J., Galeev, T. R., Harmanci, A., Kitchen, R., Bedford, J., et al. (2016a). ARTICLE A uniform survey of allele-specific binding and expression over 1000-Genomes-Project individuals. doi:10.1038/ncomms11101.

Chen, Z., Hagen, D. E., Wang, J., Elsik, C. G., Ji, T., Siqueira, L. G., et al. (2016b). Global assessment of imprinted gene expression in the bovine conceptus by next generation sequencing. *Epigenetics* 11, 501–16. doi:10.1080/15592294.2016.1184805.

Cheng, H. H., Perumbakkam, S., Pyrkosz, A. B., Dunn, J. R., Legarra, A., and Muir, W. M. (2015). Fine mapping of QTL and genomic prediction using allele-specific expression SNPs demonstrates that the complex trait of genetic resistance to Marek's disease is predominantly determined by transcriptional regulation. *BMC Genomics* 16, 816. doi:10.1186/s12864-015-2016-0.

Clark, E. L., Bush, S. J., McCulloch, M. E. B., Farquhar, I. L., Young, R., Lefevre, L., et al. (2017). A high resolution atlas of gene expression in the domestic sheep (Ovis aries). *PLOS Genet.* 13, e1006997. doi:10.1371/journal.pgen.1006997.

Daetwyler, H. D., Hickey, J. M., Henshall, J. M., Dominik, S., Gredler, B., Van Der Werf, J. H. J., et al. (2010). Accuracy of estimated genomic breeding values for wool and meat traits in a multi-breed sheep population. *Anim. Prod. Sci.* doi:10.1071/AN10096.

Degner, J. F., Marioni, J. C., Pai, A. A., Pickrell, J. K., Nkadori, E., Gilad, Y., et al. (2009). Effect of read-mapping biases on detecting allele-specific expression from RNA-sequencing data. *Bioinforma. Orig. Pap.* 25, 3207–321210. doi:10.1093/bioinformatics/btp579.

Deguchi, A., Tomita, T., Omori, T., Komatsu, A., Ohto, U., Takahashi, S., et al. (2013). Serum amyloid A3 binds MD-2 to activate p38 and NF-κB pathways in a MyD88-dependent manner. *J. Immunol.* 191, 1856–64. doi:10.4049/jimmunol.1201996.

Dewey, M. (2016). Comparison of various methods for meta–analysis of p–values. Available at: http://www.dewey.myzen.co.uk/meta/comparemet.pdf [Accessed May 8, 2018].

Dewey, M. (2018). {metap}: meta-analysis of significance values.

Edsgärd, D., Iglesias, M. J., Reilly, S.-J., Hamsten, A., Tornvall, P., Odeberg, J., et al. (2016). GeneiASE: Detection of condition-dependent and static allele-specific expression from RNA-seq data without haplotype information. *Sci. Rep.* 6, 21134. doi:10.1038/srep21134.

Fabregat, A., Jupe, S., Matthews, L., Sidiropoulos, K., Gillespie, M., Garapati, P., et al. (2018). The Reactome Pathway Knowledgebase. *Nucleic Acids Res.* 46, D649–D655. doi:10.1093/nar/gkx1132.

García-Gámez, E., Reverter, A., Whan, V., McWilliam, S. M., Arranz, J. J., Kijas, J., et al. (2011). Using Regulatory and Epistatic Networks to Extend the Findings of a Genome Scan: Identifying the Gene Drivers of Pigmentation in Merino Sheep. *PLoS One* 6, e21158. doi:10.1371/journal.pone.0021158.

Georges, M., Charlier, C., and Hayes, B. (2018). Harnessing genomic information for livestock improvement. *Nat. Rev. Genet.*, 1. doi:10.1038/s41576-018-0082-2.

GTEx Consortium, Gte., Laboratory, Data Analysis &Coordinating Center (LDACC)—Analysis Working Group, Statistical Methods groups—Analysis Working Group, Enhancing GTEx (eGTEx) groups, NIH Common Fund, NIH/NCI, et al. (2017). Genetic effects on gene expression across human tissues. *Nature* 550, 204–213. doi:10.1038/nature24277.

Guillocheau, G. M., El Hou, A., Meersseman, C., Esquerré, D., Rebours, E., Letaief, R., et al. (2019). Survey of allele specific expression in bovine muscle. *Sci. Rep.* 9, 4297. doi:10.1038/s41598-019-40781-6.

Gutierrez-Arcelus, M., Baglaenko, Y., Arora, J., Hannes, S., Luo, Y., Amariuta, T., et al. (2019). Allele-specific expression changes dynamically during T cell activation in HLA and other autoimmune loci. *bioRxiv*, 599449. doi:10.1101/599449.

Habermann, A., Schroer, T. A., Griffiths, G., and Burkhardt, J. K. (2001). Immunolocalization of cytoplasmic dynein and dynactin subunits in cultured macrophages: enrichment on early endocytic organelles. *J. Cell Sci.* 114, 229–240. Available at: http://www.ncbi.nlm.nih.gov/pubmed/11112706 [Accessed March 11, 2019].

Hach, F., Sarrafi, I., Hormozdiari, F., Alkan, C., Eichler, E. E., and Sahinalp, S. C. (2014). mrsFAST-Ultra: a compact, SNP-aware mapper for high performance sequencing applications. *Nucleic Acids Res.* 42, W494-500. doi:10.1093/nar/gku370.

Harrison, P. W., Fan, J., Richardson, D., Clarke, L., Zerbino, D., Cochrane, G., et al. (2018). FAANG, establishing metadata standards, validation and best practices for the farmed

and companion animal community. *Anim. Genet.* 49, 520–526. doi:10.1111/age.12736.

Hasin-Brumshtein, Y., Hormozdiari, F., Martin, L., van Nas, A., Eskin, E., Lusis, A. J., et al. (2014). Allele-specific expression and eQTL analysis in mouse adipose tissue. *BMC Genomics* 15, 471. doi:10.1186/1471-2164-15-471.

Hayes, B. J., and Daetwyler, H. D. (2019). 1000 Bull Genomes Project to Map Simple and Complex Genetic Traits in Cattle: Applications and Outcomes. *Annu. Rev. Anim. Biosci.* 7, 89–102. doi:10.1146/annurev-animal-020518-115024.

Hayes, B. J., Pryce, J., Chamberlain, A. J., Bowman, P. J., and Goddard, M. E. (2010). Genetic architecture of complex traits and accuracy of genomic prediction: coat colour, milk-fat percentage, and type in Holstein cattle as contrasting model traits. *PLoS Genet.* 6, e1001139. doi:10.1371/journal.pgen.1001139.

Hodgkinson, A., Grenier, J.-C., Gbeha, E., and Awadalla, P. (2016). A haplotype-based normalization technique for the analysis and detection of allele specific expression. *BMC Bioinformatics*. doi:10.1186/s12859-016-1238-8.

Huang, W. C., Ferris, E., Cheng, T., Hörndli, C. S., Gleason, K., Tamminga, C., et al. (2017). Diverse Non-genetic, Allele-Specific Expression Effects Shape Genetic Architecture at the Cellular Level in the Mammalian Brain. *Neuron* 93, 1094–1109.e7. doi:10.1016/j.neuron.2017.01.033.

Ilie, D. E., Kusza, S., Sauer, M., and Gavojdian, D. (2018). Genetic characterization of indigenous goat breeds in Romania and Hungary with a special focus on genetic resistance to mastitis and gastrointestinal parasitism based on 40 SNPs. *PLoS One* 13, e0197051. doi:10.1371/journal.pone.0197051.

Jiang, Y., Xie, M., Chen, W., Talbot, R., Maddox, J. F., Faraut, T., et al. (2014). The sheep genome illuminates biology of the rumen and lipid metabolism. *Science* 344, 1168–1173. doi:10.1126/science.1252806.

Kadarmideen, H. N., Watson-Haigh, N. S., and Andronicos, N. M. (2011). Systems biology of ovine intestinal parasite resistance: disease gene modules and biomarkers. *Mol. BioSyst.* 7, 235–246. doi:10.1039/C0MB00190B.

Kaul, S., Mittal, S. K., Feigenbaum, L., Kruhlak, M. J., and Roche, P. A. (2015). Expression of the SNARE protein SNAP-23 is essential for cell survival. *PLoS One* 10, e0118311. doi:10.1371/journal.pone.0118311.

Kijas, J. W., Lenstra, J. A., Hayes, B., Boitard, S., Porto Neto, L. R., San Cristobal, M., et al. (2012). Genome-wide analysis of the world's sheep breeds reveals high levels of historic mixture and strong recent selection. *PLoS Biol.* 10, e1001258. doi:10.1371/journal.pbio.1001258.

Kim, D., Langmead, B., and Salzberg, S. L. (2015). HISAT: a fast spliced aligner with low memory requirements. *Nat. Methods* 12, 357–360. doi:10.1038/nmeth.3317.

Larson, M. A., Wei, S. H., Weber, A. T. A., Weber, A. T. A., and McDonald, T. L. (2003). Induction of human mammary-associated serum amyloid A3 expression by prolactin or lipopolysaccharide. *Biochem. Biophys. Res. Commun.* 301, 1030–1037. doi:10.1016/S0006-291X(03)00045-7.

Li, H., and Durbin, R. (2009). Fast and accurate short read alignment with Burrows-Wheeler transform. *Bioinformatics* 25, 1754–60. doi:10.1093/bioinformatics/btp324.

Maceachern, S., Muir, W. M., Crosby, S., and Cheng, H. H. (2011). Genome-wide identification of allele-specific expression (ASE) in response to Marek's disease virus infection using next generation sequencing. *BMC Proc.* doi:10.1186/1753-6561-5-S4-S14.

Mallikarjunappa, S., Sargolzaei, M., Brito, L. F., Meade, K. G., Karrow, N. A., and Pant, S. D. (2018). Short communication: Uncovering quantitative trait loci associated with resistance to Mycobacterium avium ssp. paratuberculosis infection in Holstein cattle

using a high-density single nucleotide polymorphism panel. *J. Dairy Sci.* 101, 7280–7286. doi:10.3168/JDS.2018-14388.

Mayba, O., Gilbert, H. N., Liu, J., Haverty, P. M., Jhunjhunwala, S., Jiang, Z., et al. (2014). MBASED: allele-specific expression detection in cancer tissues and cell lines. *Genome Biol.* 15, 405. doi:10.1186/s13059-014-0405-3.

McKenna, A., Hanna, M., Banks, E., Sivachenko, A., Cibulskis, K., Kernytsky, A., et al. (2010). The Genome Analysis Toolkit: a MapReduce framework for analyzing next-generation DNA sequencing data. *Genome Res.* 20, 1297–303. doi:10.1101/gr.107524.110.

Meydan, H., Yildiz, M. A., Dodgson, J. B., and Cheng, H. H. (2011). Allele-specific expression analysis reveals CD79B has a cis-acting regulatory element that responds to Marek's disease virus infection in chickens. *Poult. Sci.* doi:10.3382/ps.2010-01295.

Montgomery, S. B., Sammeth, M., Gutierrez-Arcelus, M., Lach, R. P., Ingle, C., Nisbett, J., et al. (2010). Transcriptome genetics using second generation sequencing in a Caucasian population. *Nature* 464, 773–777. doi:10.1038/nature08903.

Mozaffari, S. V, Stein, M. M., Magnaye, K. M., Nicolae, D. L., and Ober, C. (2018). Parent of origin gene expression in a founder population identifies two new candidate imprinted genes at known imprinted regions. *PLoS One* 13, e0203906. doi:10.1371/journal.pone.0203906.

Mueller, O., Lightfoot, S., and Schroeder, A. (2004). RNA Integrity Number (RIN) – Standardization of RNA Quality Control Application. *Agil. Appl. Note, Publ. 5989-1165EN*, 1–8. doi:10.1101/gr.189621.115.7.

Nitta, T., and Takahama, Y. (2007). The lymphocyte guard-IANs: regulation of lymphocyte survival by IAN/GIMAP family proteins. *Trends Immunol.* 28, 58–65. doi:10.1016/j.it.2006.12.002.

Ocaña-Guzman, R., Vázquez-Bolaños, L., and Sada-Ovalle, I. (2018). Receptors That Inhibit Macrophage Activation: Mechanisms and Signals of Regulation and Tolerance. *J. Immunol. Res.* 2018, 8695157. doi:10.1155/2018/8695157.

Overman, R. G., Enderle, P. J., Farrow, J. M., Wiley, J. E., and Farwell, M. A. (2003). The human mitochondrial translation initiation factor 2 gene (MTIF2): Transcriptional analysis and identification of a pseudogene. *Biochim. Biophys. Acta - Gene Struct. Expr.* 1628, 195–205. doi:10.1016/S0167-4781(03)00144-1.

Pelikan, R. C., Kelly, J. A., Fu, Y., Lareau, C. A., Tessneer, K. L., Wiley, G. B., et al. (2018). Enhancer histone-QTLs are enriched on autoimmune risk haplotypes and influence gene expression within chromatin networks. *Nat. Commun.* 9, 2905. doi:10.1038/s41467-018-05328-9.

Pounds, S., and Cheng, C. (2006). Robust estimation of the false discovery rate. 22, 1979–1987. doi:10.1093/bioinformatics/btl328.

R Core Team (2017). R: A language and environment for statistical computing. Available at: https://www.r-project.org/.

Raghupathy, N., Choi, K., Vincent, M. J., Beane, G. L., Sheppard, K. S., Munger, S. C., et al. (2018). Hierarchical analysis of RNA-seq reads improves the accuracy of allele-specific expression. *Bioinformatics* 34, 2177–2184. doi:10.1093/bioinformatics/bty078.

Renfree, M. B., Hore, T. A., Shaw, G., Graves, J. A. M., Pask, A. J., Marshall Graves, J. A., et al. (2009). Evolution of Genomic Imprinting: Insights from Marsupials and Monotremes. *Annu. Rev. Genomics Hum. Genet.* 10, 241–262. doi:10.1146/annurev-genom-082908-150026.

Richard Albert, J., Koike, T., Younesy, H., Thompson, R., Bogutz, A. B., Karimi, M. M., et al. (2018). Development and application of an integrated allele-specific pipeline for methylomic and epigenomic analysis (MEA). *BMC Genomics* 19, 463.

doi:10.1186/s12864-018-4835-2.
Shi, Q., Zhuang, F., Liu, J.-T., Li, N., Chen, Y.-X., Su, X.-B., et al. (2019). Single-cell analyses reveal functional classification of dendritic cells and their potential roles in inflammatory disease. *FASEB J.* 33, 3784–3794. doi:10.1096/fj.201801489R.
Stevenson, K. R., Coolon, J. D., and Wittkopp, P. J. (2013). Sources of bias in measures of allele-specific expression derived from RNA-seq data aligned to a single reference genome. *BMC Genomics* 14, 1. doi:10.1186/1471-2164-14-536.
Suárez-Vega, A., Gutiérrez-Gil, B., Klopp, C., Tosser-Klopp, G., and Arranz, J. J. (2017). Variant discovery in the sheep milk transcriptome using RNA sequencing. *BMC Genomics* 18, 170. doi:10.1186/s12864-017-3581-1.
van de Geijn, B., McVicker, G., Gilad, Y., and Pritchard, J. K. (2015). WASP: allele-specific software for robust molecular quantitative trait locus discovery. *Nat. Methods* 12, 1061–1063. doi:10.1038/nmeth.3582.
Van den Bossche, J., Laoui, D., Morias, Y., Movahedi, K., Raes, G., De Baetselier, P., et al. (2012). Claudin-1, Claudin-2 and Claudin-11 Genes Differentially Associate with Distinct Types of Anti-inflammatory Macrophages In vitro and with Parasite- and Tumour-elicited Macrophages In vivo. *Scand. J. Immunol.* 75, 588–598. doi:10.1111/j.1365-3083.2012.02689.x.
Van der Auwera, G. A., Carneiro, M. O., Hartl, C., Poplin, R., Del Angel, G., Levy-Moonshine, A., et al. (2013). From FastQ data to high confidence variant calls: the Genome Analysis Toolkit best practices pipeline. *Curr. Protoc. Bioinforma.* 43, 11.10.1-33. doi:10.1002/0471250953.bi1110s43.
Wang, M., Hancock, T. P., Chamberlain, A. J., Vander Jagt, C. J., Pryce, J. E., Cocks, B. G., et al. (2018). Putative bovine topological association domains and CTCF binding motifs can reduce the search space for causative regulatory variants of complex traits. *BMC Genomics* 19, 395. doi:10.1186/s12864-018-4800-0.
Wickham, H., and Francois, R. (2015). dplyr: A Grammar of Data Manipulation. *R Packag. version 0.4.2.*, 3.
Wong, P. P. C., Daneman, N., Volchuk, A., Lassam, N., Wilson, M. C., Klip, A., et al. (1997). Tissue Distribution of SNAP-23 and Its Subcellular Localization in 3T3-L1 Cells. *Biochem. Biophys. Res. Commun.* 230, 64–68. doi:10.1006/BBRC.1996.5884.
Xiang, R., Hayes, B. J., Vander Jagt, C. J., MacLeod, I. M., Khansefid, M., Bowman, P. J., et al. (2018). Genome variants associated with RNA splicing variation in bovine are extensively shared between tissues Ruidong. *BMC Genomics* 19, 521. doi:10.1186/s12864-018-4902-8.
Xin, H., Lee, D., Hormozdiari, F., Yedkar, S., Mutlu, O., and Alkan, C. (2013). Accelerating read mapping with FastHASH. *BMC Genomics 2013 141* 14, S13. doi:10.1186/1471-2164-14-s1-s13.
Yamanegi, K., Yamada, N., Nakasho, K., and Nishiura, H. (2018). Participation of delta annexin A3 in the ribosomal protein S19 C-terminus-dependent inhibitory mechanism of the neutrophil C5a receptor through delta lactoferrin. *Pathol. Int.* 68, 109–116. doi:10.1111/pin.12626.
Yee, N. K., and Hamerman, J. A. (2013). β(2) integrins inhibit TLR responses by regulating NF-κB pathway and p38 MAPK activation. *Eur. J. Immunol.* 43, 779–92. doi:10.1002/eji.201242550.
Zerbino, D. R., Achuthan, P., Akanni, W., Amode, M. R., Barrell, D., Bhai, J., et al. (2018). Ensembl 2018. *Nucleic Acids Res.* 46, D754–D761. doi:10.1093/nar/gkx1098.
Zerbino, D. R., and Birney, E. (2008). Velvet: Algorithms for de novo short read assembly using de Bruijn graphs. *Genome Res.* doi:10.1101/gr.074492.107.
Zhou, Z.-Y., Hu, Y., Li, A., Li, Y.-J., Zhao, H., Wang, S.-Q., et al. (2018). Genome wide

analyses uncover allele-specific RNA editing in human and mouse. *Nucleic Acids Res.* 46, 8888–8897. doi:10.1093/nar/gky613.

Zhuo, Z., Lamont, S. J., and Abasht, B. (2017). RNA-Seq Analyses Identify Frequent Allele Specific Expression and No Evidence of Genomic Imprinting in Specific Embryonic Tissues of Chicken. *Sci. Rep.* 7, 11944. doi:10.1038/s41598-017-12179-9.

Tables

Table 1. Total number of genes with significant static ASE in proportion to genes containing informative SNVs (filtered). Tissue break-down has been presented as count (%ASE/filtered).

Sheep	Thymus	Spleen	Liver	Ileum	Total filtered	Total expressed
Female 1	-	136 (1.31%)	153 (1.47%)	92 (0.88%)	10,379	21,150
Female 2	136 (1.28%)	70 (0.66%)	116 (1.09%)	70 (0.66%)	10,572	21,420
Female 3	151 (1.22%)	75 (0.60%)	105 (0.85%)	140 (1.13%)	12,326	21,689
Avg.	143 (1.25%)	94 (0.85%)	125 (1.13%)	101 (0.89%)	11,092	21,419
Male 1	95 (0.92%)	-	157 (1.52%)	86 (0.83%)	10,282	21,361
Male 2	125 (0.99%)	54 (0.43%)	86 (0.68%)	80 (0.63%)	12,514	21,822
Male 3	106 (1.01%)	71 (0.67%)	110 (1.04%)	82 (0.78%)	10,480	21,545
Avg.	109 (0.97%)	62 (0.55%)	118 (1.08%)	83 (0.74%)	11,092	21,576
Total avg.	126 (1.13%)	78 (0.70%)	121 (1.09%)	92 (0.82%)	11,092	21,497

Table 2. Total number of genes with significant static ASE in BMDMs +/- LPS.

Sheep	BMDM 0hrs -LPS	BMDM 7hrs +LPS
Female 1	237	252
Female 2	192	233
Female 3	227	263
Female avg.	219	249
Male 1	205	193
Male 2	300	260
Male 3	260	261
Male avg.	255	238

Table 3. The variant IDs of LPS inducible ASE SNVs (Fisher's exact) and their respective genes. Data was obtained using Ensembl BioMart query builder. Highly significant SNVs are highlighted in bold (FDR< 1.0e-08)

ID	Chr	Start	End	Gene ID	Gene Name
rs418350332	1	195297663	195297663	ENSOARG00000020472	CLDN1
rs159822214	3	112164732	112164732	ENSOARG00000014876	OSBPL8
rs159926581	3	214731375	214731375	ENSOARG00000016495	-

rs159926581	3	214731375	214731375	ENSOARG00000022372	RF00221
rs159926581	3	214731375	214731375	ENSOARG00000024737	RF00593
rs159926581	3	214731375	214731375	ENSOARG00000025124	RF01151
rs159926581	3	214731375	214731375	ENSOARG00000025150	RF00593
rs193634916	4	53430934	53430934	ENSOARG00000001754	MDFIC
rs418697910	4	53430968	53430968	ENSOARG00000001754	MDFIC
rs162298949	6	92979793	92979793	ENSOARG00000018710	ANXA3
rs162298949	6	92979793	92979793	ENSOARG00000018710	ANXA3
rs160665956	9	76759747	76759747	ENSOARG00000001261	SPAG1
rs424104956	13	46654781	46654781	ENSOARG00000017292	CDS2
rs424104956	13	46654781	46654781	ENSOARG00000017292	CDS2
rs424104956	13	46654781	46654781	ENSOARG00000022618	RF00377
rs420037698	16	6887423	6887423	ENSOARG00000004700	-
rs430667535	17	50485358	50485358	ENSOARG00000017707	BRI3BP
rs430667535	17	50485358	50485358	ENSOARG00000018177	UBC
rs403064928	21	25826884	25826884	ENSOARG00000009963	SAA3
rs405439099	21	25826990	25826990	ENSOARG00000009963	SAA3
rs412192652	21	25826978	25826978	ENSOARG00000009963	SAA3
rs161531178	26	19663270	19663270	ENSOARG00000009626	MSR1

Figure captions

Figure 1. A flowchart of the allele-specific expression analysis pipeline applied to the sheep gene expression atlas dataset and optimised for WASP and GeneiASE programmes. The remapping was carried out using HISAT2 (Kim et al., 2015) in combination with SAMtools (Li et al., 2009). The Genome Analysis Toolkit v 3.8 was used for the ASE read counting section.

Figure 2. Distribution of biallelic SNVs expressed per gene in each of the 6 TxBF sheep. The total number of SNVs was averaged across thymus, liver, ileum and spleen for every animal. **A)** Histogram of SNVs per gene counts in the reference track (Ensembl in grey) and 6 sheep in red (females) and blue (males) overlaid. **B)**. The overall numbers of genes and SNVs detected in each animal (averaged over 4 tissues). **C)** Individual histograms from section A with females in red and males in blue.

Figure 3. The histogram of a global reference allelic ratio at every locus in the tissues. The distribution of ref allelic ratio showed a balanced profile without any 0 or 1 inflation which is observed in the presence of reference mapping bias. The allelic ratio above 0.51 is shown in blue and below 0.49 in red while balanced bi-allelic expression (0.49-0.51) is coloured in grey. Ref.dp = read counts for reference allele. Alt.dp = read counts for alternate allele. The y axis is square root scaled. As discussed in the text SNP that display MAE are not present in any of the samples analysed, indicating there was no inflation in either 0 or 1 allelic ratio.

Figure 4. Genes exhibiting static ASE shared across tissues from all six sheep. **A)** genes shared by four tissues with significant (FDR < 0.1) static ASE. **B)** ASE genes private to Ileum. **C)** Private to liver. **D)** Private to spleen. **E)** Private to thymus.

Figure 5. Intersectionality analysis of genes expressing significant ASE across all six sheep. In each tissue from left to right the set count of genes (dots connected by lines) illustrates the number of sheep sharing the gene. The private sets of genes are located at the far right of each graph (single dots with no line). The intersections are coloured in to illustrate the size of the set of shared genes (red [common to all 6 sheep], green [shared by 5 or 4 sheep], yellow [only in females] and purple [only in males]). Detailed lists of genes with ASE shared by at least 4 sheep are presented above each graph for **A)** Ileum, **B)** Liver, **C)** Spleen and **D)** Thymus. Two sex-specific sets of genes are highlighted: 16 genes showing ASE only in females (in yellow) and 5 genes only in males (in purple).

Figure 6. Intersection analysis of SNVs under genes with significant ICD-ASE in the BMDMs ± LPS. From left to right the set number of genes (dots connected by lines) have been illustrated in order according to the number of sheep sharing the SNV. The private sets of SNVs are located at the far right of each graph (single dots with no line).

Figure 7. Scatter plot of the adjusted p values from Fisher's exact test (unified using Stouffer unification) in BMDMs comparing expression from different alleles at 0 vs 7hrs at SNV level (LPS inducible ASE). **A)** The graph shows 646 loci exhibiting LPS inducible allelic imbalance shared across all 6 sheep. **B)** Four loci on chromosomes 3,16,17 and 21 with FDR < 1.0e-08. FDR < 1.0e-02 red line (n=16 SNVs) and FDR < 1.0e-08 blue line (n = 4 SNVs).

Figure1.

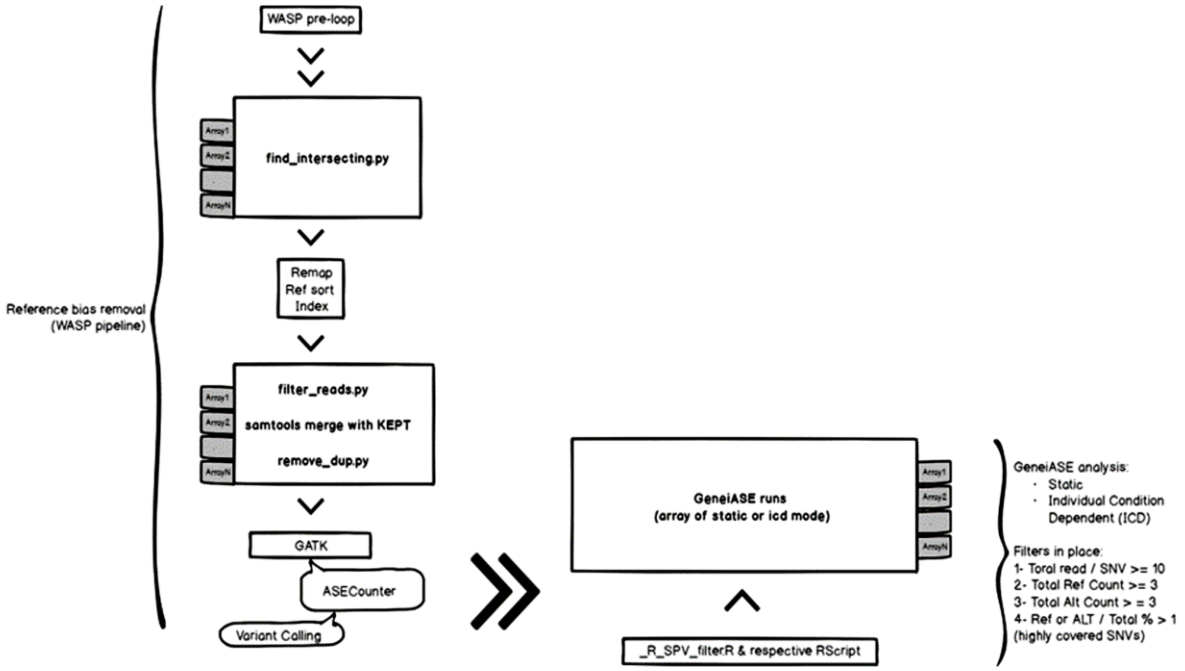

Figure2.

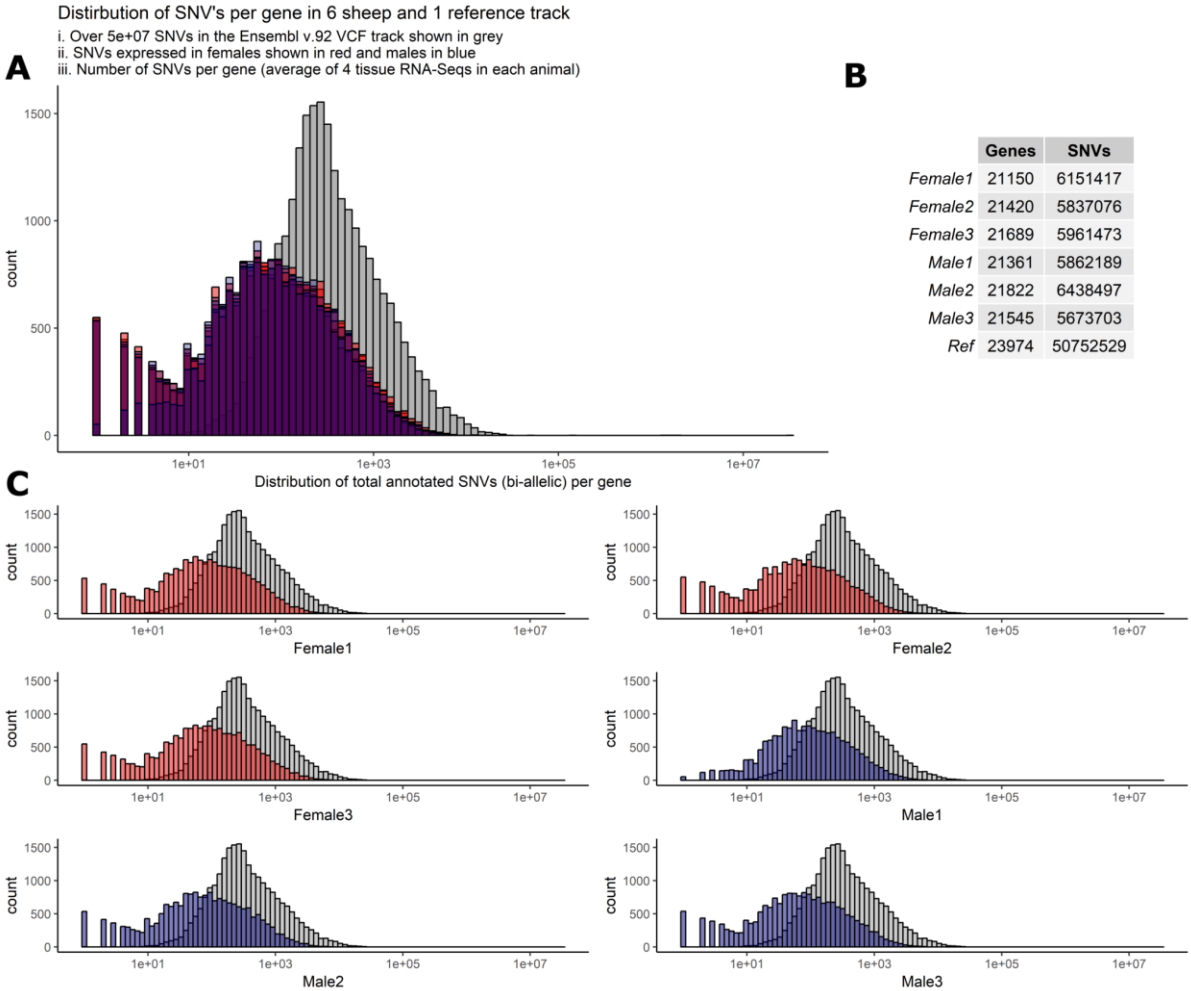

	Genes	SNVs
Female1	21150	6151417
Female2	21420	5837076
Female3	21689	5961473
Male1	21361	5862189
Male2	21822	6438497
Male3	21545	5673703
Ref	23974	50752529

Figure3.

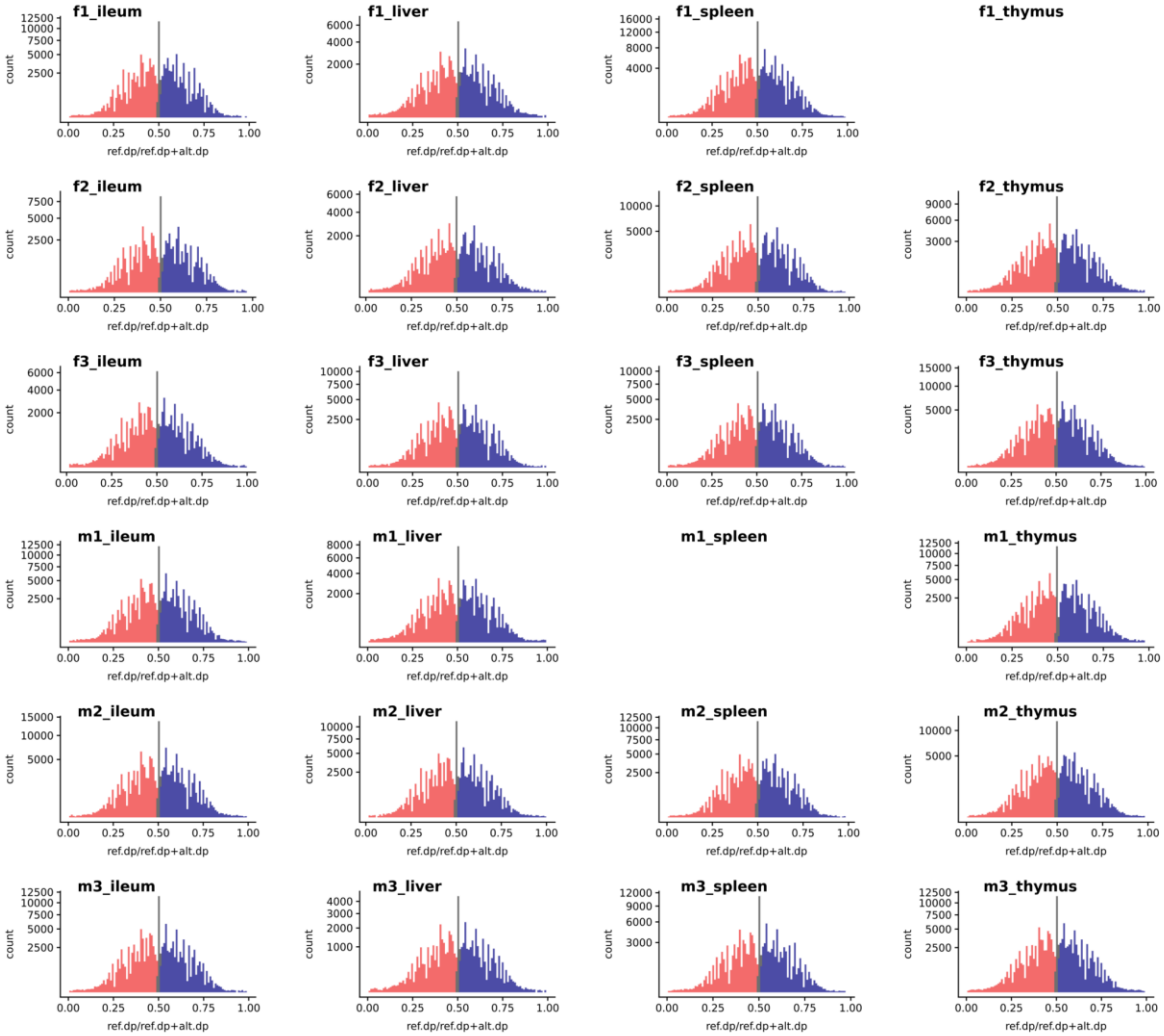
f1_ileum
f1_liver
f1_spleen
f1_thymus
f2_ileum
f2_liver
f2_spleen
f2_thymus
f3_ileum
f3_liver
f3_spleen
f3_thymus
m1_ileum
m1_liver
m1_spleen
m1_thymus
m2_ileum
m2_liver
m2_spleen
m2_thymus
m3_ileum
m3_liver
m3_spleen
m3_thymus
count
ref.dp/ref.dp+alt.dp

Figure4.

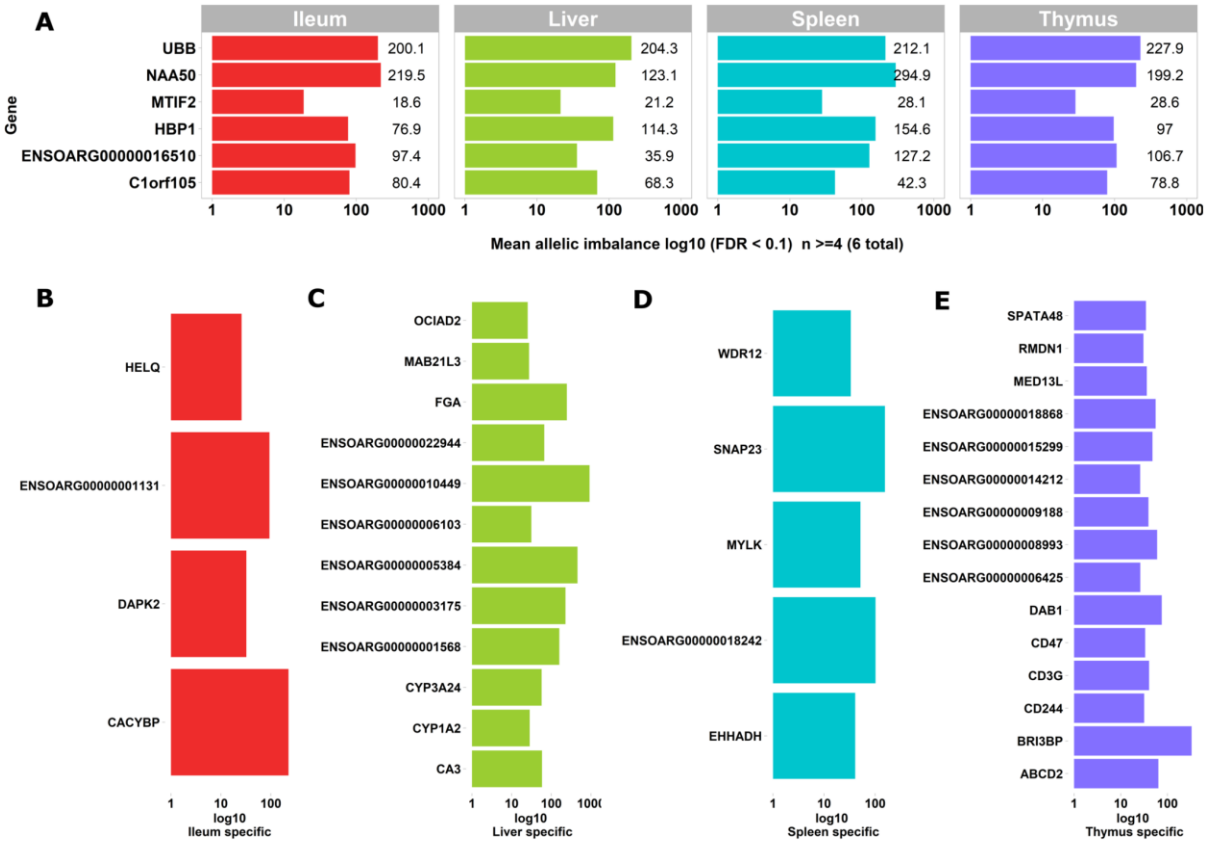
A
Ileum
Liver
Spleen
Thymus
Gene
UBB
NAA50
MTIF2
HBP1
ENSOARG00000016510
C1orf105
200.1
219.5
18.6
76.9
97.4
80.4
204.3
123.1
21.2
114.3
35.9
68.3
212.1
294.9
28.1
154.6
127.2
42.3
227.9
199.2
28.6
97
106.7
78.8
1
10
100
1000
Mean allelic imbalance log10 (FDR < 0.1) n >=4 (6 total)
B
HELQ
ENSOARG00000001131
DAPK2
CACYBP
log10
Ileum specific
C
OCIAD2
MAB21L3
FGA
ENSOARG00000022944
ENSOARG00000010449
ENSOARG00000006103
ENSOARG00000005384
ENSOARG00000003175
ENSOARG00000001568
CYP3A24
CYP1A2
CA3
Liver specific
D
WDR12
SNAP23
MYLK
ENSOARG00000018242
EHHADH
Spleen specific
E
SPATA48
RMDN1
MED13L
ENSOARG00000018868
ENSOARG00000015299
ENSOARG00000014212
ENSOARG00000009188
ENSOARG00000008993
ENSOARG00000006425
DAB1
CD47
CD3G
CD244
BRI3BP
ABCD2
Thymus specific

Figure5.

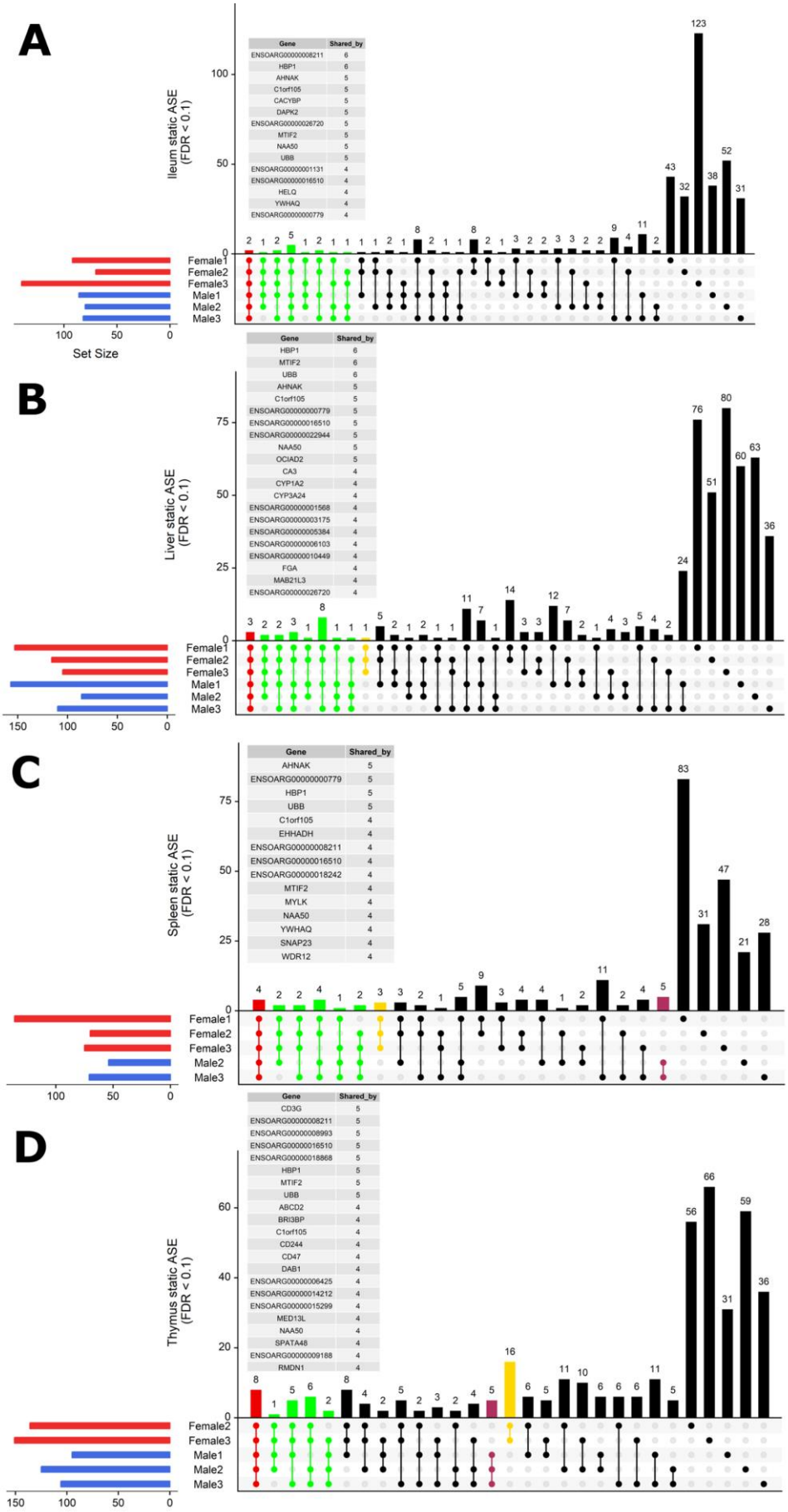
A
Ileum static ASE (FDR < 0.1)
Gene | Shared_by
ENSOARG00000008211 | 6
HBP1 | 6
AHNAK | 5
C1orf105 | 5
CACYBP | 5
DAPK2 | 5
ENSOARG00000026720 | 5
MTIF2 | 5
NAA50 | 5
UBB | 5
ENSOARG00000001131 | 4
ENSOARG00000016510 | 4
HELQ | 4
YWHAQ | 4
ENSOARG00000000779 | 4
Female1
Female2
Female3
Male1
Male2
Male3
Set Size
B
Liver static ASE (FDR < 0.1)
Gene | Shared_by
HBP1 | 6
MTIF2 | 6
UBB | 6
AHNAK | 5
C1orf105 | 5
ENSOARG00000000779 | 5
ENSOARG00000016510 | 5
ENSOARG00000022944 | 5
NAA50 | 5
OCIAD2 | 5
CA3 | 4
CYP1A2 | 4
CYP3A24 | 4
ENSOARG00000001568 | 4
ENSOARG00000003175 | 4
ENSOARG00000005384 | 4
ENSOARG00000006103 | 4
ENSOARG00000010449 | 4
FGA | 4
MAB21L3 | 4
ENSOARG00000026720 | 4
C
Spleen static ASE (FDR < 0.1)
Gene | Shared_by
AHNAK | 5
ENSOARG00000000779 | 5
HBP1 | 5
UBB | 5
C1orf105 | 4
EHHADH | 4
ENSOARG00000008211 | 4
ENSOARG00000016510 | 4
ENSOARG00000018242 | 4
MTIF2 | 4
MYLK | 4
NAA50 | 4
YWHAQ | 4
SNAP23 | 4
WDR12 | 4
D
Thymus static ASE (FDR < 0.1)
Gene | Shared_by
CD3G | 5
ENSOARG00000008211 | 5
ENSOARG00000008993 | 5
ENSOARG00000016510 | 5
ENSOARG00000018868 | 5
HBP1 | 5
MTIF2 | 5
UBB | 5
ABCD2 | 4
BRI3BP | 4
C1orf105 | 4
CD244 | 4
CD47 | 4
DAB1 | 4
ENSOARG00000006425 | 4
ENSOARG00000014212 | 4
ENSOARG00000015299 | 4
MED13L | 4
NAA50 | 4
SPATA48 | 4
ENSOARG00000009188 | 4
RMDN1 | 4
Female2
Female3
Male1
Male2
Male3

Figure6.

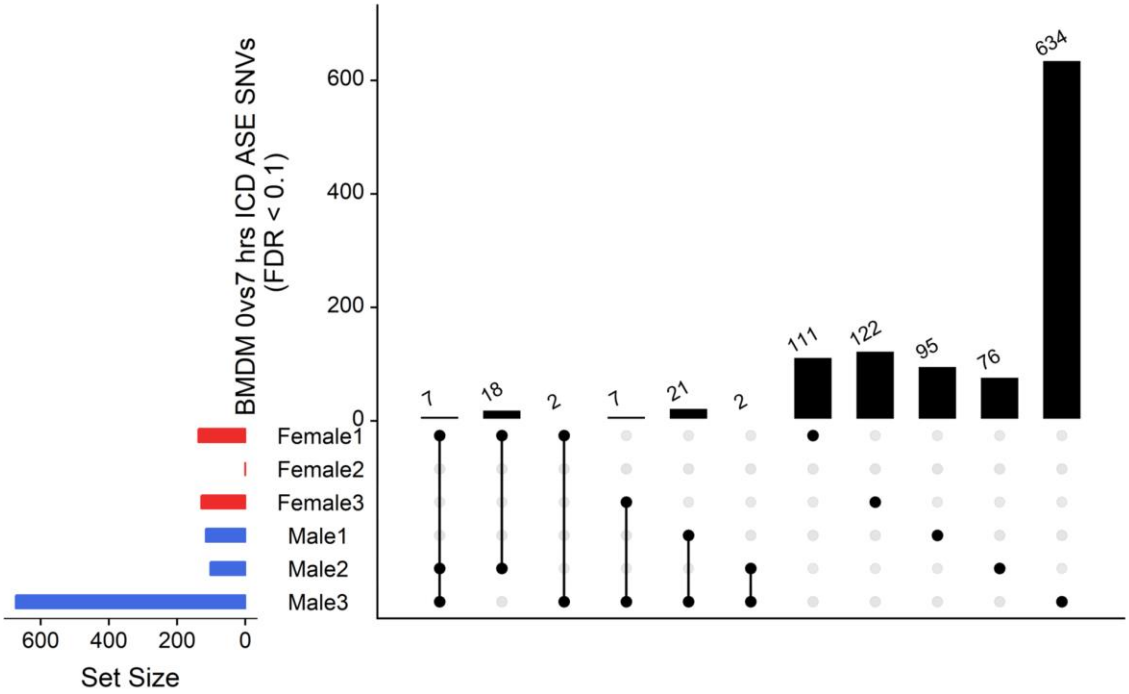

Figure 7.

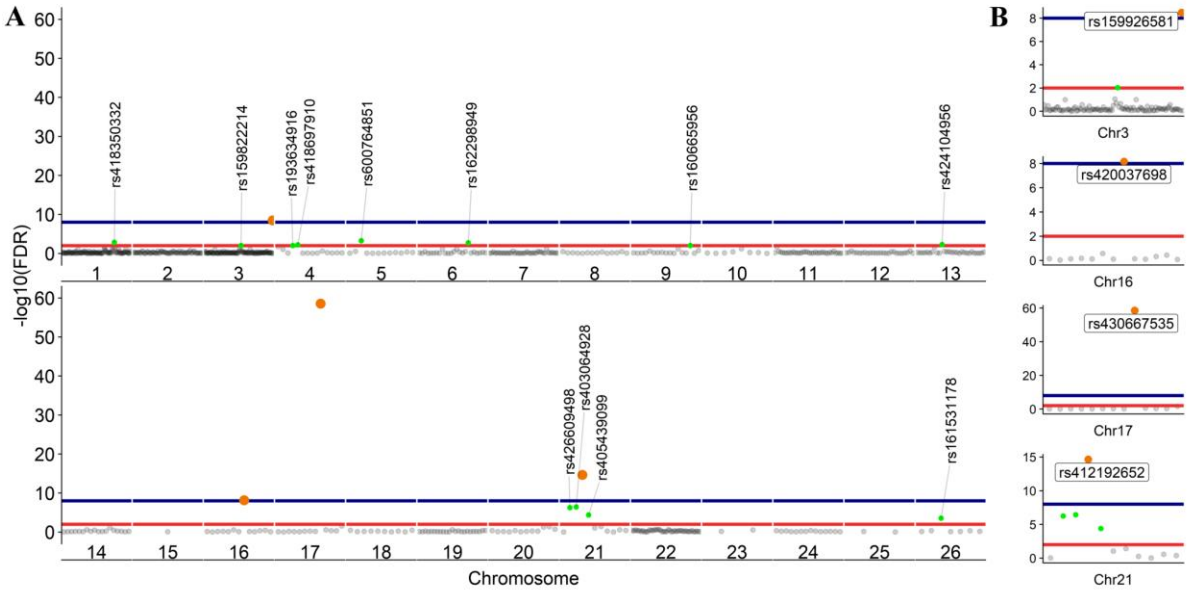

Supplementary material

Supplementary_file1.pdf

A bimodal p value distribution was observed in GeneiASE output as shown in S1 Fig.1:

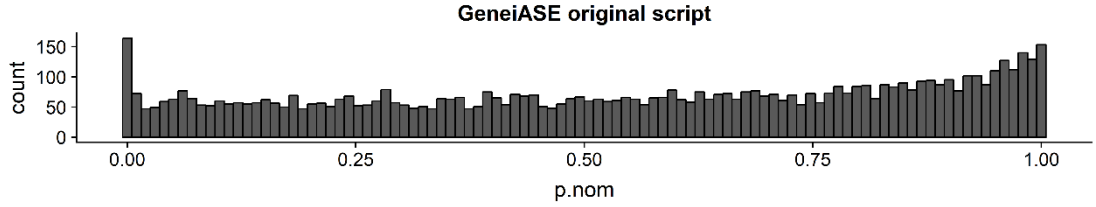

S1 Figure 1. Distribution of p values resulted from the beta-binomial test (Static ASE example for spleen in female 1). The uniformity of the p value distribution showed a bimodal (high frequency close to 1 followed by an extensive lower tail close to 0). R machine characteristics for printing float numbers were limited to 6 significant numbers after the decimal point by default which resulted in a high number of absolute zero (0+e0.0) output-values.

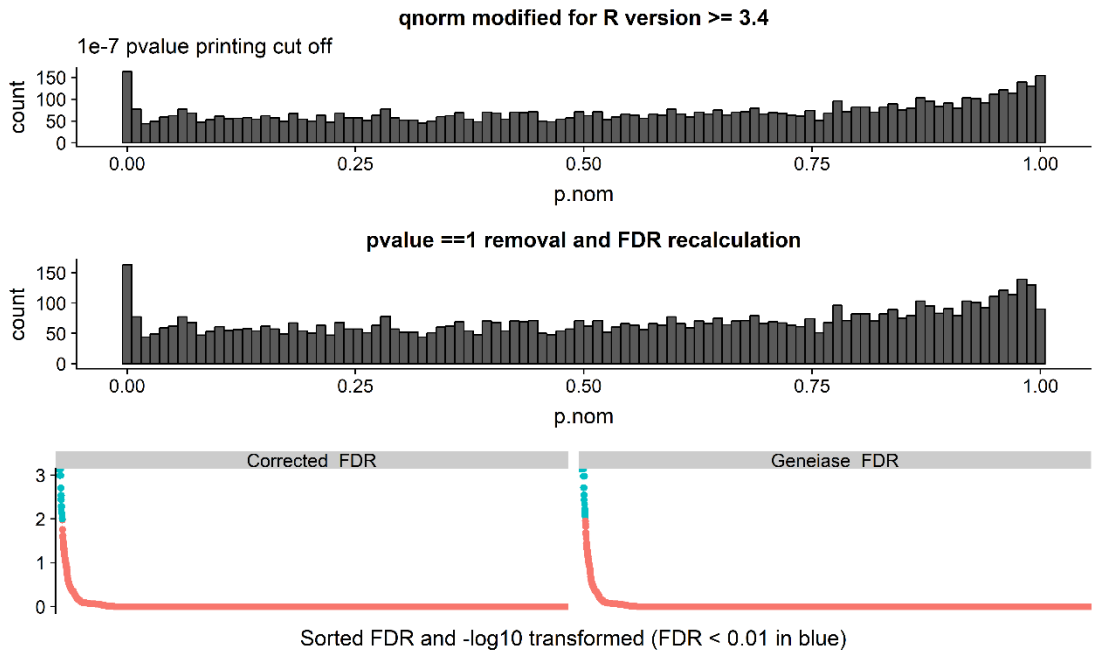

S1 Figure 2. The figure shows the distribution of p values produced by GeneiASE after cut off introduction (top) and after removal of p value == 1 values (middle). The distribution of FDR calculated by GeneiASE and after correction are shown at the bottom (right and left respectively). To correct for multiple testing by recalculation of FDR and eliminating the non-uniformity of p value distribution around 1 the following steps were performed as shown in S1 Fig.2: i) An arbitrary cut off (1e-7) was placed over all p values smaller than the said limit including the absolute 0e+0.0; ii) The genes showing p values equal to 1 were removed from each data frame; iii) The false discovery portion and rate were recalculated in each sample. iv) Gene showing FDR < 0.1 selected for further analysis.

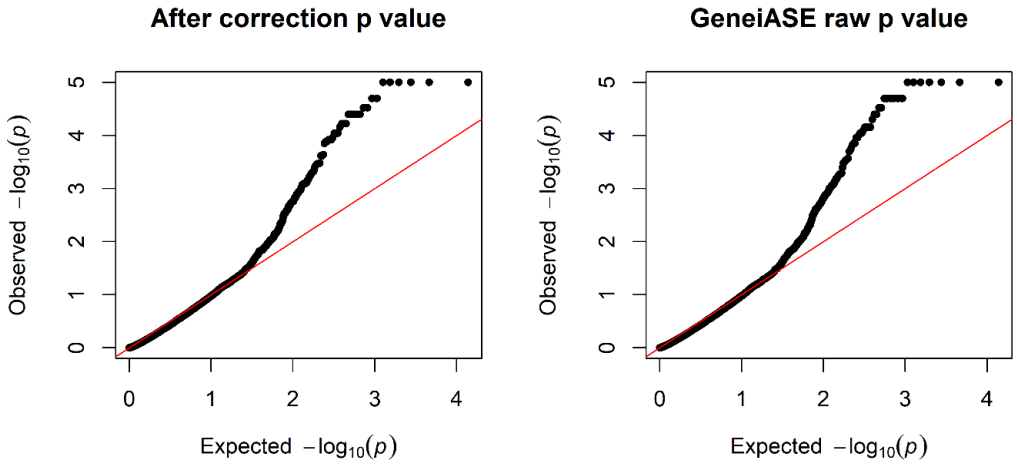

S1 Figure3. The QQ plot of observed vs expected p values in corrected (left) and GeneiASE raw (right) calculated outputs.

Supplementary_file2.zip
The zip file includes all the significant ASE values for genes and SNVs in the study.

Supplementary_file3.pdf
A

B

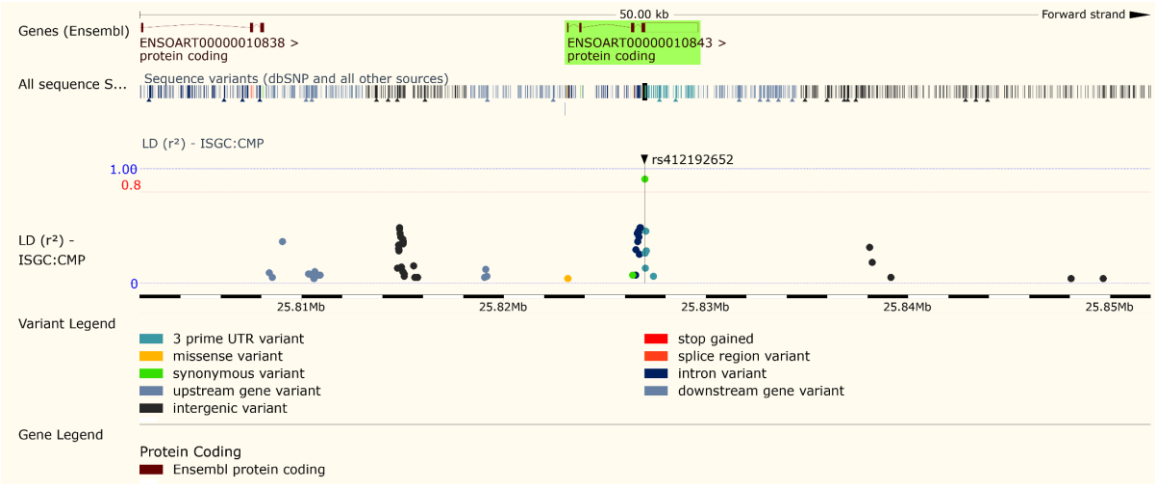

S3 Figure1. The LD block (A) and LD Manhattan plot (B) of SAA3 transcript (ENSOART00000010843). The LD block produced as part of International Sheep Genome Consortium is publicly available on Ensembl using the COMPOSITE population (n = 98).

Supplementary_file4.pdf

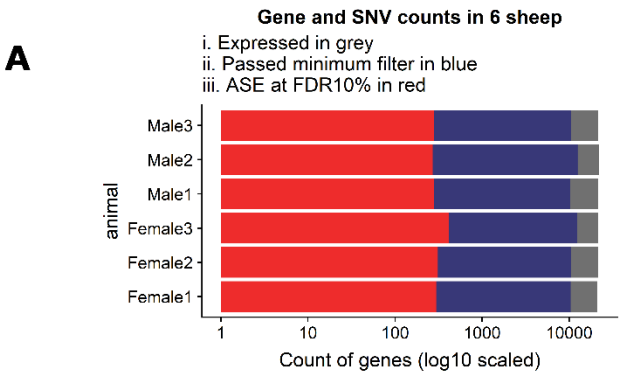

B

animal	Feature	Expressed	Filtered	ASE
Female1	gene	21150	10379	297
Female1	snv	6151417	125210	5985
Female2	gene	21420	10572	310
Female2	snv	5837076	109205	7095
Female3	gene	21689	12326	417
Female3	snv	5961473	137852	10811
Male1	gene	21361	10282	279
Male1	snv	5862189	125651	6740
Male2	gene	21822	12514	271
Male2	snv	6438497	151451	7110
Male3	gene	21545	10480	279
Male3	snv	5673703	115660	6558

S4 Figure 1 supp to Figure 2. The proportional distribution of SNVs being expressed, passing minimum filtration criteria and showing significant ASE (FDR 10%). A) Count of genes in 6 sheep expressed in grey, informative/filtered in blue and ASE positive in red. B) Break down of genes and SNVs that are expressed, pass minimum filtration criteria and are ASE positive.

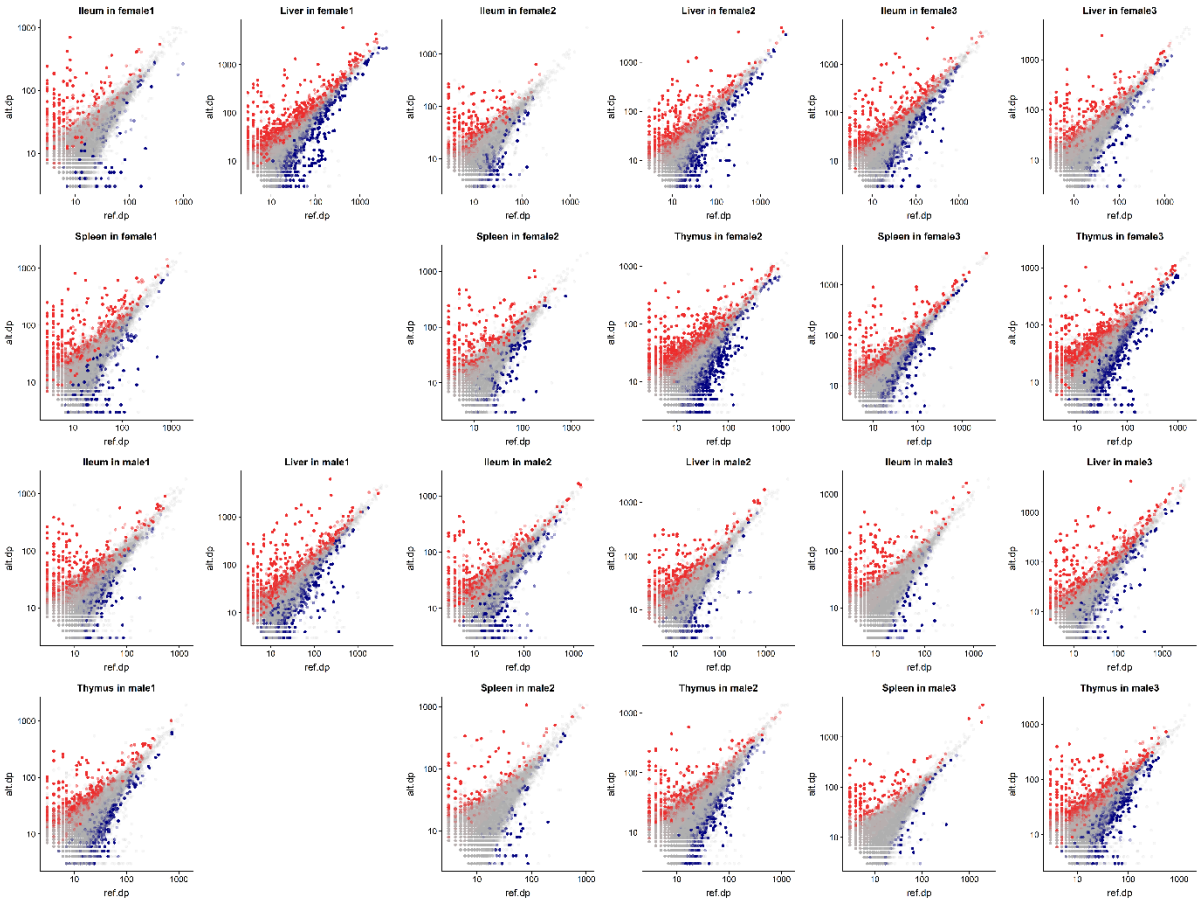

S4 Figure 2 supp to Figure 3. Scatter plot of allelic depth (read count) in all 4 tissues of the 6 TxBF sheep. The SNVs passing minimum filtration criteria are coloured in grey and significant ASE (FDR10%) are marked by red and blue. If reference read count > alternate read count the point is shown in blue and vice versa in red. Expression level varies across tissues but does not affect the ASE profile.

S4 Table 1 supp to Figure 6. Mean allelic imbalance (log2(ASE_{+LPS}/ASE_{-LPS})) in all 6 sheep. Only 1 gene (VCAN including 7 SNVs) exhibited inducible ASE which was shared between 3 sheep (in bold), while two (GCNT1 and SYNE3) showed inducible ASE in two sheep. Diverse and highly individual ASE response to LPS was observed in each sheep.

Gene	Female1	Female2	Female3	Male1	Male2	Male3
ACOD1	-	-	-	6.8	-	-
ASH2L	-	-	-	-	3.9	-
CASP8	-	-	-	-	-	9.8
CCDC80	-	-	9.1	-	-	-
CLDN1	-	-	-	-	-	10.3
CPOX	-	-	-	-	-	6.5
EDNRB	-	-	-	-	-	11.4
EMP1	-	-	-	-	-	23.9
ENSOARG00000001174	-	-	-	-	5.0	-
ENSOARG00000001910	-	-	-	-	-	7.8
ENSOARG00000002108	-	-	-	-	-	8.0
ENSOARG00000002898	-	-	-	-	-	5.3
ENSOARG00000004106	-	-	-	-	-	7.5
ENSOARG00000006889	-	-	31.9	-	-	-
ENSOARG00000007547	-	-	-	-	8.2	-
ENSOARG00000007603	-	-	-	6.9	-	-
ENSOARG00000014875	-	-	-	-	-	5.6
ENSOARG00000016081	6.4	-	-	-	-	-
ENSOARG00000018177	-	-	11.0	-	-	-
ENSOARG00000021562	-	-	-	-	-	9.0
FDX1	-	-	-	-	17.3	-
GCNT1	-	-	-	16.9	-	30.4
GSDME	-	-	-	4.6	-	-
HNMT	-	-	-	-	-	15.1
HUNK	-	-	-	-	-	4.0
IL1RN	-	-	-	-	-	9.7
KANSL1L	-	-	-	-	-	4.7
KMO	-	-	-	-	-	9.7
MB21D2	-	-	-	5.3	-	-
MYO10	-	-	-	-	-	7.8
NRP1	-	-	9.3	-	-	-
OGFRL1	-	-	-	-	-	16.5
PDE4D	-	-	-	-	-	11.7
PDK4	-	-	-	6.9	-	-
PGM2	-	-	-	-	-	9.5
PLK2	-	-	-	-	-	6.7
PPIF	6.9	-	-	-	-	-
PRNP	-	-	-	-	-	8.8
RASSF3	-	-	-	-	9.2	-

RGS1	-	-	-	-	-			8.4
SAFB2	-	-	-	-	-			5.3
SIGLEC15	-	-	-		4.8	-	-	
SLC35F2	-	-	-	-		6.5	-	
SYDE1	-	-	-	-	-			5.1
SYNE3	-	-		7.2	-	-		10.7
TBC1D1	-	-	-		6.3	-	-	
TFEC	-	-		10.3	-	-	-	
TRAF1	12.1	-	-	-	-	-	-	
VCAN	23.5	-	-	-		14.0		13.9
VLDLR	-	-	-	-		4.7	-	

f